1-1-2014

# Cytogenetic Evaluation Of Low Dose Hyper-Radiosensitivity In Human Lymphoblastoid Cell Lines Exposed To Cobalt-60 Gamma Radiation.

Gnanada Sameer Joshi
*Wayne State University,*

# CYTOGENETIC EVALUATION OF LOW DOSE HYPER-RADIOSENSITIVITY IN HUMAN LYMPHOBLASTOID CELL LINES EXPOSED TO COBALT-60 GAMMA RADIATION

**by**

**GNANADA S. JOSHI**

**DISSERTATION**

Submitted to the Graduate School

of Wayne State University,

Detroit, Michigan

in partial fulfillment of the requirements

for the degree of

**DOCTOR OF PHILOSOPHY**

2014

MAJOR: BIOLOGICAL SCIENCES

Approved by:

_____

Advisor Date

_____

_____

_____

## DEDICATION

This work is dedicated to my husband, Sameer Joshi, for his endless love and selfless support. I also dedicate this work to my three beautiful children, Atharv, Aryan and Aditi for their unconditional love and innocent support. This work would not be possible without all the encouragement and motivation I received from my family.

## ACKNOWLEDGEMENTS

The past five years in graduate school have been an amazing experience. I have had an opportunity to work with a great group of people from all over the world, diverse in their scientific knowledge, culture and values. I have learnt much from each one of them, for which I will always be thankful to the Graduate School.

I am very privileged to have worked with Dr. James D. Tucker, who is an excellent mentor. I am very thankful for the confidence he has always showed in me during my most difficult days while in the program. Most of all, I will always be obliged to him for training me with interviewing and personnel management skills, which were an extremely important part of my Ph.D. The confidence he has instilled in me to identify the right people for the job and successfully complete a project by making the best use of the unique skills of each worker, are beyond the scope of any Ph.D. I will forever be confident and proud to carry these skills with me in addition to the scientific experience that I have gained in his laboratory, for which I will always remain indebted to him.

I am extremely thankful to each of my committee members, Dr. Michael C. Joiner, Dr. Victoria Meller and Dr. Athar Ansari for their guidance and support through my scientific quest. I would specially like to thank Dr. Joiner for his help with irradiations and the discussions about various aspects of my projects despite his busy schedule. Dr. Meller has always been very interested about my work and her queries during the various committee meetings have helped me gain better insights into my research area - Thank you! I would like to specially thank Dr. Ansari for being very approachable and supportive through my difficult times in graduate school.

Learning is at its best in a healthy competitive and encouraging environment for which I would like to thank all my colleagues at the Tucker lab: Dr. Robert Thomas, Dr. Rohan Kulkarni, Dr. Raj Asur, Dr. Will Grever, Sountharia Rajendran, Ramya Loganathan, Nicole Bailey, Hilary Moale, Erica Call, Anita Chalasani, Tamara Briazova, Gaila Pirockinaite, Kyle Polasek, Mark Krycia, Angie Bustamante, Margaret Leone, Han Cheong, and especially Isheeta Seth and Marina Bakhmutsky for their support and friendship. I would specially like to thank Dr. Rohan Kulkarni for being an excellent support and a great friend at all times.

The most treasured non-scientific experiences at the Tucker lab include training and working with a large group of undergraduate students. I am thankful to Batoul Aoun, Luis Balderas, Stephanie Barry, Zaven Bush, Amanda Croskey, Robert Flinn, Lauren Gibbons, Darryl Goodyear, Cam Ha, Sarah Hassan, Jennifer Jiles, Justin L'Esperance, Kyle Mangan, Abbey McKinney, Kaitlin McKinney, Antonela Muca, Anisa Musleh, Maher Musleh, Yara Najjaraltinawi, John Permaloff, Richard Raad, Jonathan Salamon, Hatim Shafiq, Jordan Sharon, Amy Szczepanski, Malati Vadapalli and Daniel Zukowski for their efforts, without which my projects would have never been completed.

I would like to thank the office personnel at the Department of Biological Sciences for their help with numerous tasks and paper work. I also thank the Graduate School for the financial support through their Graduate Enhancement Research funds.

I would like to thank the people who make my life worthy of living, my family and friends. I would specially like to thank Arti Dhiraaj for her support and unconditional friendship. My deepest gratitude to my parents, Late Mrs. Jayashree Kulkarni and Mr. Suresh Kulkarni for instilling persistence and good values that are the basis of my

personality. I would like to thank my parents-in-law, Mrs. Nanda Joshi and Mr. Avinash Joshi for their immense support and everlasting confidence in me. I would like to thank my brother, Mr. Krishna Prasad Kulkarni and my brother-in-law, Col. Tushar Joshi and their families for constant support. My three children, Atharv, Aryan and Aditi, have been ”constructive” distractions that were most needed in difficult times; I thank them for their unconditional love. Lastly, I am extremely thankful to my husband, Mr. Sameer Joshi, for his patience, support and constant encouragement. This work was impossible without him!

## TABLE OF CONTENTS

## LIST OF TABLES

## LIST OF FIGURES

# CHAPTER 1

# INTRODUCTION

## Ionizing Radiation

Ionizing radiation results in the removal of electrons from the orbit of an atom or molecule, thereby forming unstable ions. The resulting ionized molecules can cause direct damage to DNA leading to single or double strand breaks. Single strand breaks are comparatively easy to repair since the undamaged DNA strand serves as a template. Double strand breaks cause DNA rearrangements which lead to more severe biological consequences resulting in cell cycle arrest, senescence, or cell death.

## Radiation types and properties

To understand the biological effects of radiation exposure, a basic understanding of radiation physics is needed. Ionizing radiation can consist of atomic or subatomic particles such as alpha and beta particles, and protons and neutrons, which all have mass, or photons (X-rays and γ-rays) that have properties of high energy electromagnetic waves. γ-rays are characterized as low linear energy transfer (low-LET) radiation (Hill 2004). LET refers to the amount of energy transferred along the linear path of radiation in matter such as tissue. The energy transferred by X-rays and γ-rays results in less ionization along their paths and less homogeneous ionization within the cells than particles such as protons, neutrons, and α-particles which deposit more energy per distance travelled, and are therefore considered to be high-LET radiation. Radiation dose is measured in Gray (Gy), which is defined as the energy absorbed per unit mass. One Gray of ionizing radiation is equivalent to 1 joule of energy absorbed per

kilogram of matter (J/kg). One way to assess the risks of cancer arising from exposure to a particular radiation source is to measure the biological effects per unit of dose absorbed by the matter, which is often expressed in Sieverts (Sv). The overall aim of the current study was to understand the biological consequences of exposures to low doses of γ-rays.

**Damaging effects of radiation**

Much of our knowledge of the human health consequences of radiation exposure is due to studies that focused on the effects of the atomic bombs detonated over Hiroshima and Nagasaki in 1945 (Cronkite et al. 1955; Bond and Cronkite 1957; Little 2009; Douple et al. 2011). The biological consequences of exposure to radiation have also been well documented in studies performed on cleanup workers from the 1986 nuclear power plant accident at Chernobyl, Ukraine (Moore et al. 1997; Moore and Tucker 1999; Jones et al. 2002). In addition to war and accident survivors, epidemiological studies on radiation workers (Cardis et al. 1995; Tucker et al. 1997; Sont et al. 2001; Cardis et al. 2007; Leung et al. 2011; Ostroumova et al. 2014) and radiotherapy patients (Kleinerman et al. 2005; Curtis RE FD 2006; Leung et al. 2011) have provided much information on the actual biological damage post exposure. The detrimental effects of the consequences of the atomic bombings in Japan and the Chernobyl accident are due to high-energy electromagnetic waves that interact with the cells and displace electrons, causing damage to biomolecules and thus inducing oxidative stress. At high acute doses (> 1 Gy), both direct and indirect damage to cells is severe and will affect most of the cellular processes including DNA damage repair.

However, at low doses (< 1 Gy), repair of direct and indirect DNA damage is initiated but may be inefficient in restoration of the damage, thereby resulting in point mutations and DNA rearrangements.

Relatively high doses in humans lead to Acute Radiation Syndrome (ARS). There are three distinct classical syndromes of ARS. The first is bone marrow (or hematopoietic) syndrome, which results in destruction of bone marrow leading to a weakened immune system and increased hemorrhage. The hematopoietic syndrome is observed even with acute radiation exposures as low as 0.7 Gy and is very severe at 10 Gy. The second is gastrointestinal (GI) syndrome, which causes damage to the GI tract leading to vomiting, nausea, severe dehydration, and death within a few weeks. GI syndrome is due to radiation exposures that are approximately 6 Gy. Finally, the cardiovascular (CV) / central nervous system (CNS) syndrome is caused by extremely high dose exposures of 20 - 50 Gy. An exposure to such severe acute doses results in the collapse of the circulatory system and increased pressure in the brain due to accumulation of fluids. The CV / CNS syndrome results in death in a few hours or days due to severity of its symptoms (Reeves 1999). An important consideration is that different doses cause different specific features of ARS in different organs, reflecting their radiosensitivities.

**Human exposures to radiation**

As stated earlier, human exposure to high doses of radiation have occurred mostly due to war or accidents, as evidenced in the atomic bomb explosions in Japan and the Chernobyl nuclear power plant accident in Ukraine. The unfortunate natural disaster leading to the meltdown of nuclear material at the Fukushima Daiichi nuclear

power plant in Japan in 2011 is currently causing tremendous concern because the radiation levels have been reported to be very high in parts of the surrounding area. Some kinds of fruits and vegetables, milk and water in regions in and near Daiichi are reported to have radioactivity much above the background radiation.

We are constantly exposed to radiation by a variety of natural and artificial sources. Natural background radiation sources include radioactive elements found in the water and food, radon gas released from the earth's crust, and cosmic rays. According to the United Nations Scientific Committee on the Effects of Atomic Radiation (UNSCEAR), the global average radiation dose from natural background radiation is approximately 2.4 mSv per year (UNSCEAR 2000; Mettler et al. 2007). The annual dose from natural background radiation varies depending upon location, with some areas emitting significantly higher doses of radiation, for example, Ramsar in Iran, Kerala in India, Guarapari in Brazil, northern Flinders Range in Australia, and Yangjiang in China. Within the United States, the National Council on Radiation Protection (NCRP) monitors the amount of radiation exposure to the general population. The NCRP has reported that the current average global effective radiation dose is approximately 3.0 mSv per year, however their recent reports indicate that these values have almost doubled and are now considered to be about 5.7 mSv per year, which includes all radiation sources (NCRP 2009). This difference between the radiation exposures is not due to changes in the natural sources but due to increased medical radiological procedures, as shown in Table 1.1. These procedures were for most part considered "safe" for many years, however many studies have demonstrated chromosome damage at doses below 0.5 Gy exposures (Tucker et al. 1998; Bhatti et al. 2010).

**Table 1.1. Average effective annual radiation dose from current standard medical procedures***

| **Medical Procedure** | **Approximate effective annual radiation dose (mSv)** |
|---|---|
| Radiography (X-ray) - GI Tract | 6.0 – 8.0 |
| Radiography (X-ray) – Spine | 1.5 |
| Radiography (X-ray) - Extremity | 0.001 |
| Radiography (X-ray) - Chest | 0.1 |
| Radiography (X-ray) - Dental | 0.005 |
| Computed Tomography (CT) -Abdomen and Pelvis | 15 - 30 |
| Computed Tomography (CT) – Colonography | 10 |
| Computed Tomography (CT) - Head | 2 – 4 |
| Computed Tomography (CT) - Spine | 6 |
| Computed Tomography (CT) - Chest | 1.5 - 7 |
| Mammography | 0.4 |

*Modified from www.radiologyinfo.org/en/safety/index.cfm?pg=sfty_xray; accessed on 08/20/2014.

The American population's exposure to increasing amounts of radiation for medical imaging has raised concerns over the increased cancer risk from diagnostic radiology, especially that of Computed Tomography (CT) scanning (Brenner and Hall 2007). Brenner and Hall proposed that this increase in the CT scanning alone raises cancer risk by 1.5 – 2%. Bhatti et al. (Bhatti et al. 2010) demonstrated significant increases in chromosome translocations, even in healthy individuals, post exposure to X-rays performed annually. The Bhatti et al. and Brenner et al. studies emphasize that long term health risks associated with low dose radiation exposures are currently under-estimated and thus need to be further investigated.

**Biological effects at low dose exposures**

A program focusing on the biological effects of low dose exposures by the U.S. Department of Energy identifies low dose radiation as exposures ≤ 20 cGy (http://lowdose.energy.gov/default.aspx), which are considerably higher than the natural background radiation levels. However, evaluating long-term effects of exposures at low doses and achieving accurate risk analyses is difficult since the ultimate concern stemming from radiation exposure is cancer, which may be caused due to additional factors such as age and life style choices (Fuglede et al. 2011; Srivastava et al. 2011). Therefore, the risks of exposure to low doses are currently estimated based on data obtained at high doses. With continued exposure to radiation through medical imaging systems, a larger population in general is exposed to doses that are above natural background radiation (Table 1.1). Therefore, a clear understanding of the risks involved

at low doses is needed for a meaningful risk-reward analysis of such radiation exposures.

The current method for low dose risk assessment is linear-no-threshold (LNT) extrapolation from the high dose data, which is an approach that has been used for the past 50 years (ICRP 1991). According to the LNT hypothesis, risk is directly proportional to radiation dose (Rothkamm and Lobrich 2003). The LNT models further propose the "dose additivity" concept, which suggests that radiation-induced DNA damage accumulates over time and increases the risk of carcinogenesis (Mitchel 2007). However, an increasing amount of evidence questions the validity of the LNT models.

Two alternatives to the LNT models are the linear threshold models and the hormesis and adaptive response models. The linear threshold models suggest that below a certain threshold there is no detectable risk (Tanooka 2001; Pierquin et al. 2007). According to the hormesis and adaptive response models, low levels of radiation exposure prior to a high dose can actually reduce the risks of radiation-induced cellular damage (Yonezawa et al. 1990; Day et al. 2007; Sethu et al. 2008; Jeggo 2009) and are therefore in direct opposition to the "dose additivity" tenant of the LNT models. In contrast, the non-targeted radiation-induced bystander effect amplifies the radiation response in unirradiated cells leading to an increased risk at low doses that is unpredicted by the LNT models (Hamada et al. 2006; Little 2006; Prise 2006). Thus, accurate assessments of risks from low dose radiations are essential for the development of adequate radiation exposure limits imposed by governments.

**Cellular responses to low-dose exposures**

Radiation exposure leads to breaks in the double helix and can potentially cause cancer. At the same time, radiation also provides powerful tools for treating cancers. The dual role of radiation, in both causing DNA damage as well as its therapeutic benefits, is due to the intricate molecular pathways triggered. Cellular responses to DNA damage depend on the cell and tissue type (Helleday et al. 2008; Kinner et al. 2008) as well as the nature and magnitude of the damage (Gudkov and Komarova 2007).

Improvements in cell survival assays have also been important for studying low dose phenomena such as hyper-radiosensitivity (HRS) (Marples and Collis 2008). HRS can be described as an increased sensitivity of cells in G2 phase to low dose radiation and has been observed in a wide range of cell types and tissues (Joiner et al. 1993; Marples and Joiner 1993; Wouters et al. 1996; Ryan et al. 2008). At doses in the range of 0 – 30 cGy, mammalian cell survival assays display HRS as a steep slope of the dose response curve that is a result of increased cell death at these doses. For slightly higher doses, in the range 30 – 60 cGy, an induced radiation resistance (IRR) effect is observed wherein cells display increased survival (Figure 1.1).

The mechanisms underlying HRS / IRR are not completely understood. At low doses the early G2/M checkpoint is not completely activated, suggesting the involvement of ataxia telangiectasia mutated (ATM) kinase (Bakkenist and Kastan 2003; Buscemi et al. 2004; Lobrich and Jeggo 2005; Wykes et al. 2006; Krueger et al. 2010; Martin et al. 2013). In the absence of the G2 / M checkpoint, cells with damaged DNA enter mitosis leading to cell death. Some studies have also shown that the HRS effect translates to increased apoptosis for low doses (Enns et al. 2004; Krueger et al. 2007b).

Interestingly, the HRS / IRR-related effect is also observed in various tissues (Joiner and Johns 1988; Joiner et al. 2001b). However, a better explanation of the HRS / IRR effect is required to help estimate actual damage caused at low doses. This will help obtain better analyses of the risks involved for improved treatment options.

Chapter 2 of this dissertation describes the work performed to evaluate radiation-induced G2-specific HRS effects at 0 – 20 cGy in four normal human lymphoblastoid cell lines using cytogenetics. Based on the clonogenic cell survival data from other studies (Marples and Collis 2008; Martin et al. 2013), we hypothesized that the slope of the response curve at very low doses (line “C” in Figure 1.2) will be greater than the extrapolated curve (line “B” in Figure 1.2). We provide cytogenetic evidence of HRS in all four cell lines tested in this study (Chapter 2). Prior to conducting this work, there was the possibility that the slope of the response would be lower than the extrapolated curve (line “D” in Figure 1.2). The results shown here strongly support the expectation of the slope being greater than the extrapolated data, and argue strongly against the alternate hypothesis of the slope being less than that derived by extrapolation.

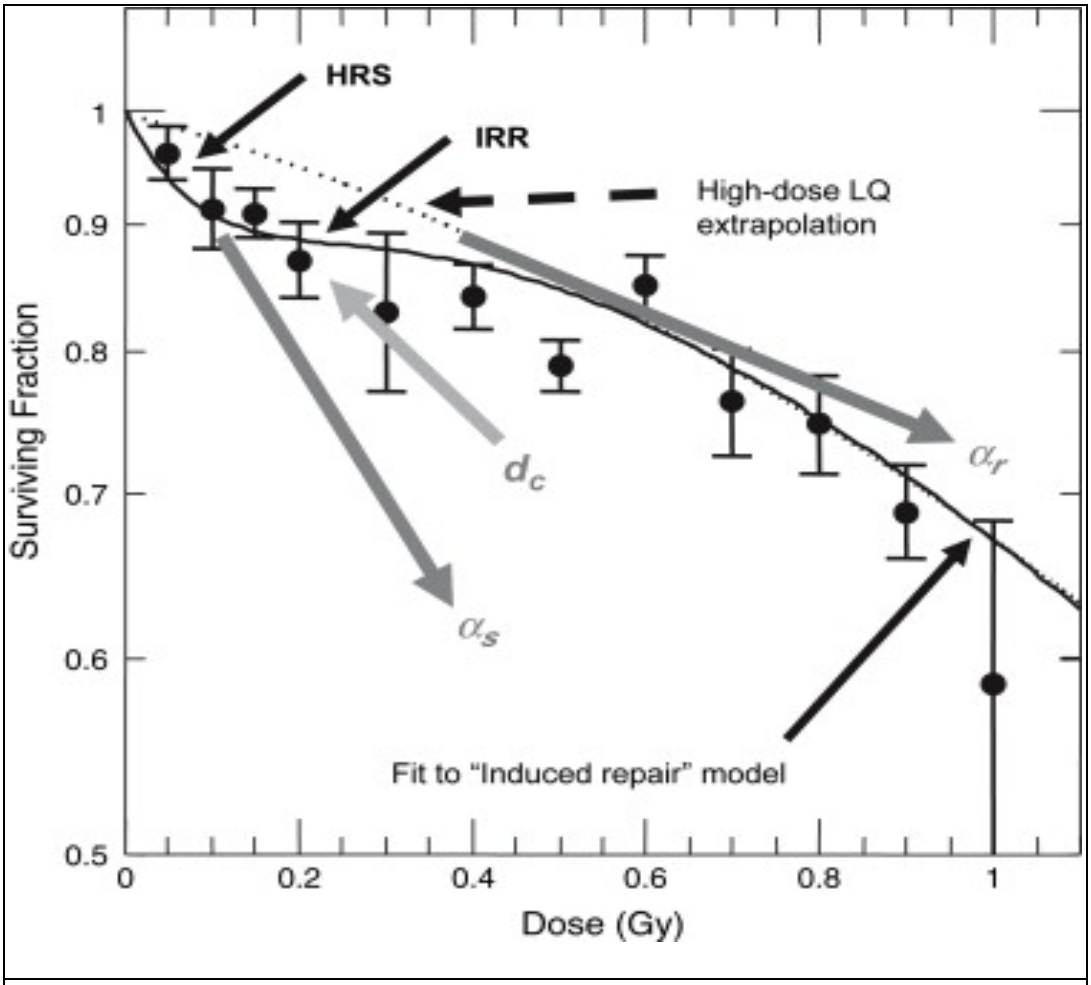


**Figure 1.1** Clonogenic cell survival curve below 100 cGy. At doses from 0 – 30 cGy, mammalian cells demonstrate hyper-radiosensitivity (HRS), and show induced radiation resistance (IRR) between 30 and 60 cGy. The current method of risk analyses at low dose exposures is to extrapolate the data obtained from the high doses (above 1 Gy). However, due to the HRS/IRR effect, extrapolation does not consider the changes in the typical cell survival curves for radiation-induced sensitivity ($\alpha_s$) or resistance ($\alpha_r$) as indicated here. This image was obtained from Marples et al., (Marples and Collis 2008).

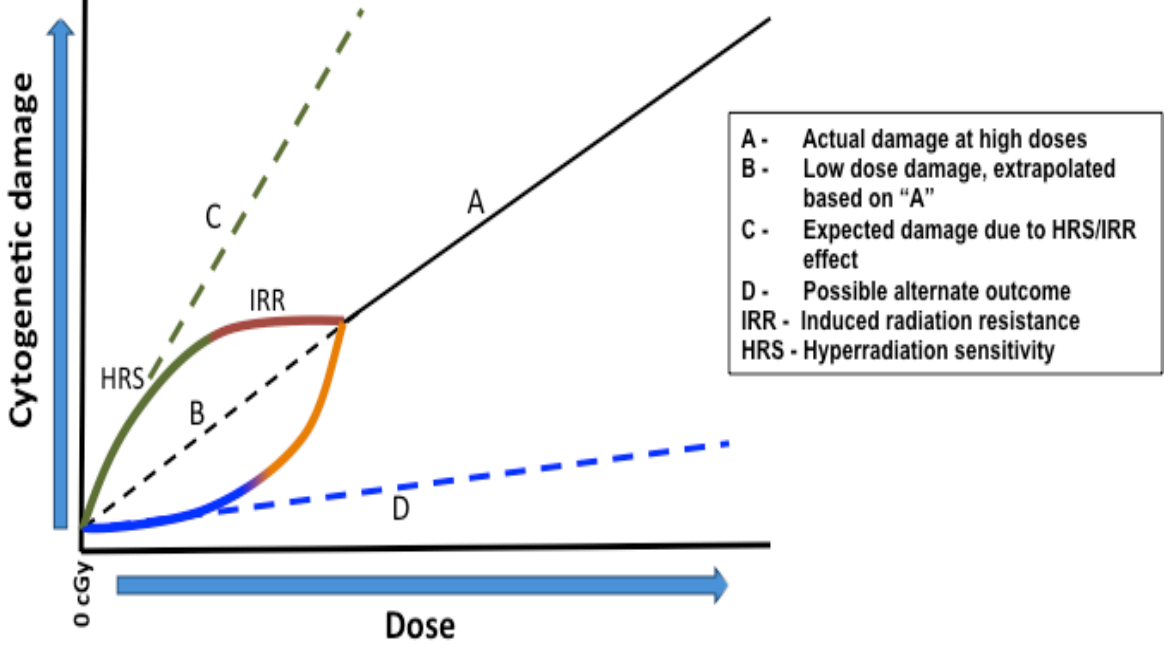


**Figure 1.2.** Possible response curves at low doses. Cytogenetic damage increases with amount of radiation based on high dose exposures (A). At low doses the damage has sometimes been estimated by extrapolating the response from the high doses (B); this is the approach used by Linear No Threshold models. Outcome C is strongly supported by the cytogenetic evidence of the HRS, which is discussed in Chapter 2. The alternate outcome D is currently not supported by literature.

**Effect of oxygen ($O_2$) levels on radiation responses**

Most *in vitro* radiobiological experiments are conducted under ambient atmospheric $O_2$ levels (~21%), a value that exceeds the *in vivo* physiological $O_2$ levels (~5%) by about four-fold in most normal tissues. $O_2$ levels may even be lower than 5% in some solid tumor microenvironments. Compared to cells grown at physiological $O_2$ levels, culturing cells in ambient $O_2$ results in increased intracellular amounts of hydroxyl ions that result in DNA strand breaks (Henderson and Miller 1986; Boregowda et al. 2012; Koukourakis 2012). With hypoxic conditions there are fewer DNA strand breaks and these appear to be repaired efficiently due to activation of ATM and ATR mediated DNA repair pathways (Cam et al. 2010; Mongiardi et al. 2011; Stagni et al. 2014). The biological effects of radiation are highly influenced by $O_2$ levels, with hypoxia and anoxia making cells two to three times more resistant to radiation (Palcic et al. 1982; Marples et al. 1994b; Hockel and Vaupel 2001; Ma et al. 2013). Tumor hypoxia, especially before radiotherapy, is known to be associated with poor clinical prognosis (Semenza 2012). Hypoxia is related to tumor development, metastatic capacity and malignant progression, and results in resistance to therapy at doses above 1 Gy (Brown et al. 2010; Hanahan and Weinberg 2011; Song et al. 2011).

Many solid tumors often have areas with inadequate circulation due to structurally disorganized blood vessels and because of cells that replicate faster than the developing tumor capillary network (Hockel and Vaupel 2001; Brown 2002; Rockwell et al. 2009). The fraction of solid tumors that are hypoxic (with $O_2$ levels below physiological conditions), and the degree of hypoxia in tumors, vary considerably (Moulder and Rockwell 1987; Teicher et al. 1995). Tumors display two types of hypoxia,

1) chronic hypoxia due to limited diffusion of oxygen in tissues as a result of impaired tissue vasculature and 2) acute hypoxia, due to poor blood perfusion in the existing blood vessels (Vaupel and Harrison 2004). Both chronic and acute tumor hypoxia lead to induced radioresistance (Garcia-Barros et al. 2003). Radiation resistance is partly due to increased DNA repair and decreased apoptosis due to activation of hypoxia inducible factors (Robertson et al. 2009; Aypar et al. 2011). Thus, poor tumor oxygenation directly results in failure of the radiation treatment (Hockel et al. 1993; Parker et al. 2004; Rockwell et al. 2009). Therefore, true cellular radiation responses may be masked or distorted by an unnaturally high level of oxidative lesions imposed by atmospheric $O_2$. In Chapter 3 we explored the consequences of low $O_2$ levels on irradiated normal human lymphoblastoid cells. In addition to the low $O_2$ levels, we also evaluated the consequences of post-radiation re-oxygenation to ambient air and post-irradiation hypo-oxygenation. Our results call into question the soundness of the *in vitro* experimental methods used for understanding radiation-induced cellular damage in human cells cultured in ambient air.

**DNA repair processes**

DNA damage detection and repair is required for normal cell development and survival. Radiation-induced double-strand breaks cause DNA rearrangements ultimately affecting cell survival (Noda et al. 2012). Thus, radiosensitivity of the cells depends on their capacity to repair the damaged DNA and varies among cells. Increased radiosensitivity is evident in cancer patients with mutations in repair enzymes such as ATM, resulting in a high fraction of cell killing (Thompson 2012). Thus, the response to

damage is crucial for the cells to divide and proliferate, or die. In addition to the initiation of the repair processes, the “quality” of repair is also important for the DNA to be functional. For example, the detection of DNA double strand breaks by ATM can initiate repair mechanisms which in turn leads to the activation of the tumor suppressor gene p53 (Canman and Lim 1998). The p53 protein plays an important role in controlling cell cycle arrest and also acts as a pro-apoptotic enzyme that by stimulating caspase activity leads to cell death by apoptosis (Thompson 2012; Han et al. 2014).

The repair of DNA double strand breaks is either accomplished via homologous recombination repair (HRR) or non-homologous end joining (NHEJ). HRR utilizes the corresponding undamaged DNA on the sister chromatid as a template for repairing the damage, resulting in perfect repair (Thompson 2012; Symington 2014). In the NHEJ repair the DNA strands are ligated, ignoring the missing base pairs in the process (Mahaney et al. 2009), thus causing the loss of some genetic information ultimately resulting in translocations and telomere fusions (Thompson 2012). DNA repair that is not functional or adequate can lead to mitotic catastrophe that in turn results in cell death.

Progression through the cell cycle is also important when considering radiosensitivity. Cells exhibit differential radiosensitivity in different cell cycle phases, being sensitive in G2-M and resistant in late S phase (Terasima and Tolmach 1963). One possible explanation for this radiation resistance in S phase is that the sister chromatid is opened and readily accessible for homologous repair of DNA double strand break. The potential long-term impact of radiosensitivity based on cell-cycle phases post-radiation is explored in Chapters 2 and 3.

**Cytogenetic analyses of chromosome damage**

Ionizing radiation is known to cause damage to DNA. Classical cytogenetic analyses of chromosome aberrations are considered to be the gold standard for biological dosimetry. The cytokinesis-blocked micronucleus (CBMN) assay is a commonly used, fast, simple, and sensitive cytogenetic method which can efficiently identify three different endpoints simultaneously, namely micronuclei (MN), nucleoplasmic bridges, and nuclear buds.

Radiation-induced MN are derived from acentric chromosomes, chromatid fragments, or lagging whole chromosomes that did not attach to the spindle fibers during nuclear division and hence were excluded from the daughter nuclei. These fragments and lagging chromosomes are enclosed in a nuclear membrane forming one or more MN (Figure 1.3, A and B) (Eastmond and Tucker 1989b; Albertini et al. 2000; Fenech et al. 2011). Nucleoplasmic bridges are formed when the centromeres of dicentric chromosomes become attached to spindle fibers from opposite poles during nuclear division. The nuclear membrane develops around the daughter nuclei as well as the dicentric chromosome(s) resulting in one or more nucleoplasmic bridges (Figure 1.3, C and D). The mechanisms of formation of nucleoplasmic buds are not well understood.

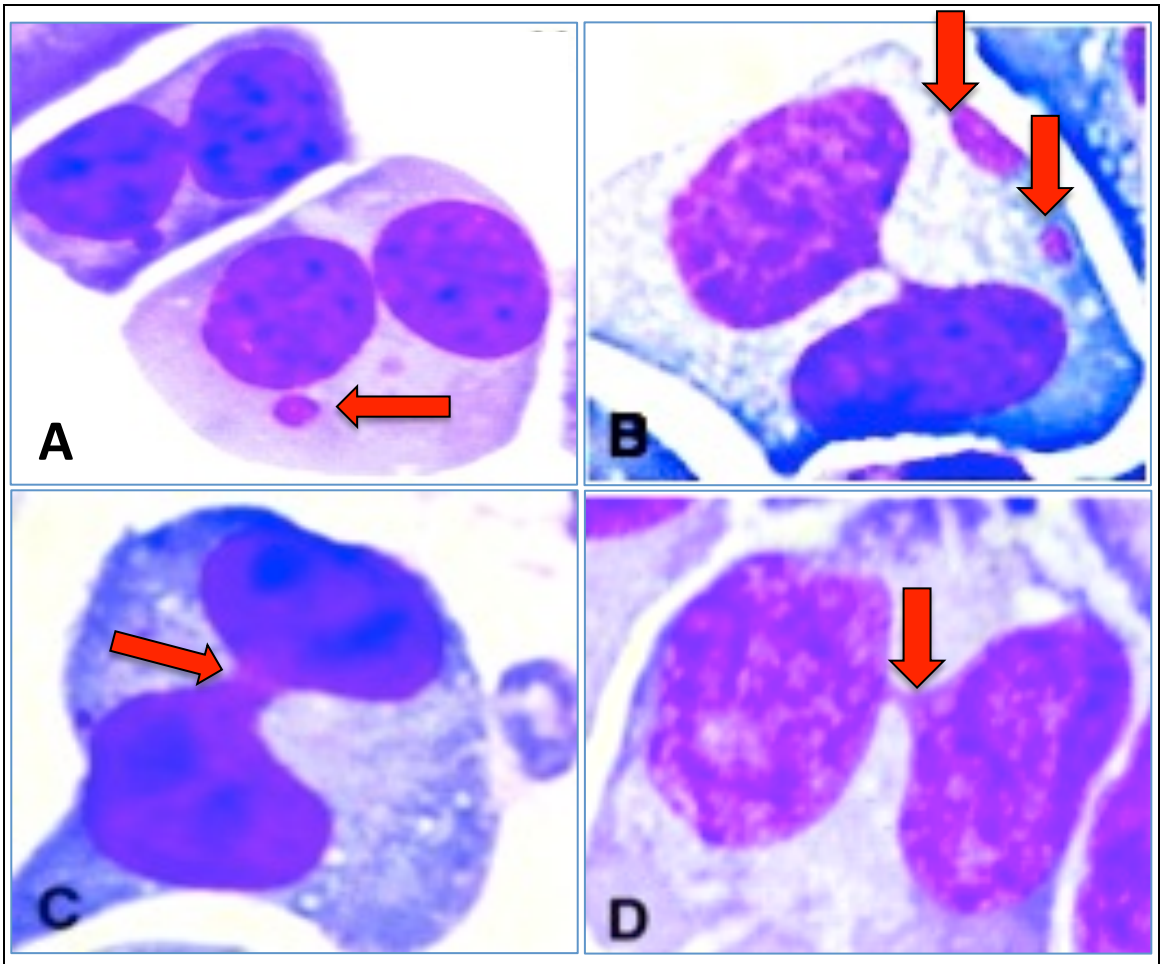


**Figure 1.3**. Images of Giemsa stained binucleated cells with micronuclei (**A** and **B**) and nucleoplasmic bridges (**C** and **D**).

A commonly used cytokinesis blocking agent is Cytochalasin B, which inhibits polymerization of actin filaments, thus preventing the formation of the microfilament ring which constricts the cytoplasm during the cell division leading to formation of binucleated cells (Fenech 2000). The MN and bridges expressed in the cytokinesis-blocked binucleated cells are easily scored to enumerate chromosome damage (Fenech 2000; Fenech et al. 2003). We used the CBMN assay and specifically evaluated the frequencies of MN and bridges as cytogenetic endpoints for the studies described in Chapters 2 and 3. The data for nuclear buds did not yield any meaningful results and for this reason were excluded from further analyses in both studies.

# CHAPTER 2

## Cytogenetic characterization of low-dose hyper-radiosensitivity in Cobalt-60 irradiated human lymphoblastoid cells

## INTRODUCTION

Radiation-induced damage and the associated cancer risks are well known for high doses, however substantial uncertainty still exists about the health risks associated with low-dose exposures (Pierce and Preston 2000; Brenner et al. 2003; Scott 2008; Morgan and Bair 2013). Human exposure to radiation has increased considerably over the past few decades due to more frequent use of CT imaging and radiological procedures. Currently the estimates of the biological damage at low-dose exposures are based on linear extrapolation of the available high dose (> 100 cGy) data. However at low-dose exposures (≤ 100 cGy), radiation responses have been observed to deviate from linearity (Zaichkina et al. 2004; Scott 2008).

Clonogenic cell-survival assays involving mammalian cells exposed to X-rays have identified hyper-radiation sensitivity (HRS) effects, where increased cell death is observed at low doses (≤ 50 cGy) accompanied by induced radiation resistance (IRR) at slightly higher doses (≥ 60 cGy) (Joiner et al. 1996; Wouters and Skarsgard 1997; Joiner et al. 2001a; Marples and Collis 2008; Martin et al. 2013). HRS has been investigated for increased tumor cell killing as a way to treat cancer and might also protect normal tissues against carcinogenesis following low-dose radiation exposures (Lambin et al. 1994). The potential clinical significance of HRS is not well understood (Martin et al. 2013), and the mechanisms underlying the HRS/IRR effect are unclear. However, evidence suggests that faithful DNA repair and effective cell cycle regulation may be diminished at very low doses (Marples et al. 2004; Krueger et al. 2010).

Radiation-induced DNA damage triggers activation of checkpoints in the G1/S, S, and G2 phases of the cell cycle which allow time for repair of damaged DNA before cell cycle progression recommences (Wilson 2004). The HRS/IRR effect is predominantly observed in G2 (Joiner et al. 1996; Short et al. 2003; Marples 2004), suggesting that the rapidly occurring G2 cell cycle checkpoint regulates the mechanisms of the HRS/IRR effect. During G2, radiation-induced DNA damage is verified by two distinct cell cycle checkpoints, one which arrests cells that have incurred damage in G1 or S (Sinclair 1968) and the other (called the rapid G2/M check point) is triggered when cells in G2 are exposed to radiation (Xu et al. 2002). The rapid G2/M checkpoint depends on the ataxia telangiectasia mutated (ATM) protein and is known to activate at ≥ 40 cGy (Xu et al. 2002; Krempler et al. 2007). Thus, cells exposed to doses below 40 cGy in G2 may fail to recognize the damage and enter mitosis before adequate DNA repair occurs, thereby exhibiting an HRS effect (Short et al. 2003; Wykes et al. 2006; Krueger et al. 2007a; Marples and Collis 2008).

Here we investigated cells exposed to Cobalt-60 gamma rays in G2 by comparing the slopes of the dose-responses for micronuclei and nucleoplasmic bridges in the low-dose region (< 50 cGy) to responses at higher doses (> 60 cGy). The data for four independent normal human lymphoblastoid cell lines indicate that cells irradiated in G2 with doses ≤ 20 cGy show increased cytogenetic damage per unit dose compared to doses of 60 cGy and higher, and thus exhibit an HRS effect. We also evaluated the shape of the dose-responses of the G2 irradiated cells and compared them to the responses of the G1 irradiated cells for all four cell lines. The data indicate that at low doses, the responses of the G2 irradiated cells deviate from linearity, thus suggesting

that back-extrapolation of the high dose responses may lead to underestimates of the actual damage. These findings suggest that the increased cell killing in the HRS region of G2 irradiated cells seen by others reflects the cytogenetic damage observed here, emphasizing the importance for better understanding of the HRS effect and the influence it can have on radiation risk assessments following low-dose exposures.

# MATERIALS AND METHODS

## Cell lines and cell culture

Four normal human lymphoblastoid cell lines GM15036, GM15510, GM15268, and GM15526 obtained from the Coriell Cell Repository were used in this study. The cells were cultured based on a standard protocol provided by Coriell. Briefly, the cells were grown in T-25 flasks (ISC BioExpress, Kaysville, UT) containing 10 ml of RPMI1640 medium (GIBCO, Grand Island, NY and Hyclone, Logan, UT) supplemented with 15% Fetal Bovine Serum (FBS, Atlanta Biologicals, Lawrenceville, GA), 2 mM L-glutamine (GIBCO, Grand Island, NY), penicillin-streptomycin (100 units/ml penicillin G Sodium, 100 µg/ml streptomycin sulfate in 0.85% saline) (GIBCO, Grand Island, NY) and fungizone (amphotericin B, 2.5 µg/ml, 0.2 µm filtered) (Hyclone, Logan, UT) with loosened caps. Cell cultures were maintained at 37°C and 5% $CO_2$ in a fully humidified incubator, and passaged every three to four days when their density reached $10^6$ cells/ml.

## Irradiation

Twenty-four hours after seeding the flasks, the cells were acutely exposed to Cobalt-60 γ-radiation at a dose rate of approximately 28 cGy/min at the Gershenson Oncology Center, Wayne State University, Detroit, MI. Each cell line was individually exposed to 0, 5, 10, 20, 40, 60, 80, 100, 200, 300, or 400 cGy. Each experiment was independently replicated once for each cell line.

**Cell cycle kinetics and harvest**

To measure cell cycle kinetics, flow cytometric analyses were performed on GM15036 and GM15510 cells by the Flow Cytometry Core facility, Wayne State University. The length of the G2 phase in GM15510 and GM15036 cells was determined to be approximately 1.5 and 2 hours, respectively, and the cell cycle durations were approximately 20 and 22 hours for GM15510 cells and GM15036 cells, respectively. The harvest times were based on these results to ensure that most binucleated cells scored were in G2 to observe a hyper-radiation sensitivity / induced radiation resistance (HRS/IRR) effect (Joiner et al. 1993) or in G1 for the comparison experiments.

The growth rates of GM15268 and GM15526 cells were determined by a cell viability assay, using 0.4% Trypan blue (in phosphate buffered saline; Fisher Scientific, Pittsburg, PA). Briefly, cells were seeded at an initial concentration of $3x10^5$ cells per ml and cultured as described above. An aliquot of cells was taken every 24 hours and the number of live cells per ml was determined using a standard hemocytometer (Fisher Scientific, Pittsburg, PA). The growth kinetics of both the GM15268 and GM15526 cells were comparable to those of GM15510 and GM15036, thus the harvest times were established as 2 and 22 hours after radiation to probe the G2 and G1 phases, respectively.

**Cytokinesis-blocked micronucleus (CBMN) assay**

Cytogenetic damage was measured using the CBMN assay. Immediately following irradiation, 6 µg/ml of Cytochalasin B (final concentration; Sigma Aldrich, St.

Louis, MO) was added to the flasks, which were immediately returned to the incubator. At harvest, the cells were resuspended and spun onto ethanol-cleaned microscope slides using a cytocentrifuge (Statspin, Westwood, MA) at 1300 rpm for 4 minutes. The slides were air dried, fixed in 100% methanol (Fisher Scientific, Pittsburgh, PA) for 15 minutes, stained with 10% Giemsa (Sigma Aldrich, St. Louis, MO) dissolved in water for 15 minutes, then briefly rinsed in water and air-dried.

**Data collection**

Slide readers were extensively trained prior to data collection. An equal number of readers scored equivalent numbers of cells for each treatment condition for all four cell lines, both replicates and both harvest times (G1 and G2). To ensure that adequate numbers of binucleated cells were available after irradiation, the nuclear division index (NDI) was calculated as described (Eastmond and Tucker 1989a). For each treatment condition, 200 cells were counted to determine the frequency of cells with 1, 2, 3 or 4 nuclei using the formula

$$NDI = (M_1 + 2M_2 + 3M_3 + 4M_4) / N$$

where $M_1$ to $M_4$ represent the number of cells with 1 to 4 nuclei and N is the total number of cells scored.

**Cell scoring criteria**

The slides were evaluated for micronuclei, nucleoplasmic bridges and buds simultaneously, based on established criteria (Fenech 2000; Cheong et al. 2013) using Nikon Eclipse E200 light microscopes at 1000X magnification. As shown in Figure 2.1,

all cells scored were binucleated where the two main nuclei were separate from each other and the cell membranes were intact. The micronuclei were required to be one-third the size of the main nuclei or smaller, smooth edged, round or oval, stained similar to the main nuclei, and had to be located within the cytoplasm. The nucleoplasmic bridges were required to be colored similar to the nuclei and to be connected to both nuclei. Although buds were scored, they were relatively infrequent and did not yield meaningful results, so these data are not reported here. All slides were coded prior to scoring to avoid observer bias. At least 1000 binucleated cells were scored for each treatment condition.

**Statistical analyses**

The dependence of cytogenetic damage on dose was evaluated to characterize the HRS/IRR effect by comparing the responses in G1 and G2, and to evaluate the shape of the responses of G2-irradiated cells with those of the G1-irradiated cells. The slopes of the responses were evaluated by performing univariate linear regression analyses independently on each cell line and replicate, and by multivariate linear regression analyses on the combined data for both replicates and all four cell lines using JMP software, version 6.0, SAS Institute Inc. For univariate analyses the frequencies of MN and bridges per 1000 binucleated cells were independently regressed against dose. For multivariate analyses the frequencies of MN and bridges per 1000 binucleated cells were evaluated in linear regression models using dose, cell line, cell cycle phase, experimental replicate, and an interaction term for

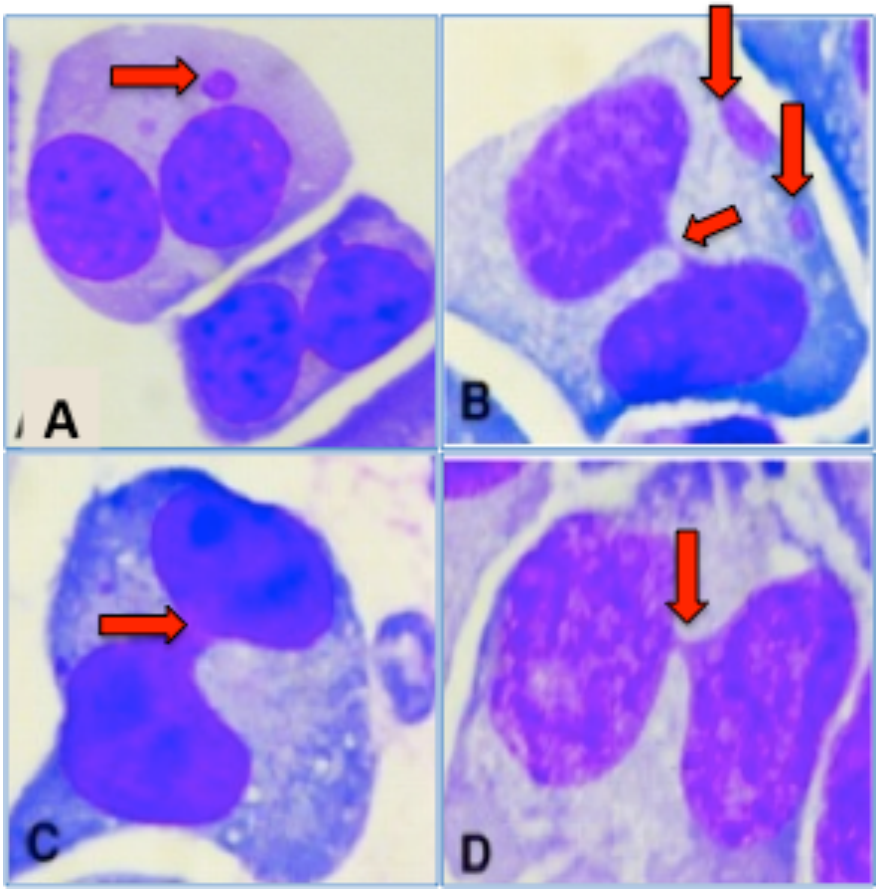


**Figure 2.1.** Examples of MN and bridges in binucleated cells. A: cell with one MN. B: cell with two MN and a bridge. C: cell with a broad bridge. D cell with thinner bridge.

cell line and replicate. The individual slopes obtained at the low- and the high-dose regions for the G2 and G1 responses were compared by calculating their ratios.

Radiation sensitivity per unit dose for MN and bridges was measured by calculating the slope of the line obtained between the frequency at the 0-cGy control and the frequency at each individual radiation dose. These individual slope values were then plotted against dose.

## RESULTS

Cytogenetic damage for MN and bridges was assessed in normal human lymphoblastoid cells irradiated with 0 – 400 cGy in G1 and G2. The results demonstrate the existence of a non-linear response in G2 for doses <100 cGy, and a clear evidence of the HRS effect < 20 cGy. In the final analyses the 400 cGy data were excluded because the frequencies of micronuclei and bridges were often lower than in cells exposed to 300 cGy. Inclusion of the 400 cGy data would have decreased the slopes of the high-dose responses leading to artificial increases in the ratios of low- to high-dose slopes, which would have exaggerated the apparent HRS effects. The frequencies of MN and bridges seen at 400 cGy likely underestimate the actual cytogenetic damage for two reasons. First, multiple acentric fragments can be packaged into one micronucleus, and multiple dicentrics may contribute to one bridge. Second, heavily damaged cells would be less likely to survive long enough to be evaluated.

### Nuclear division indices (NDI)

NDI were individually calculated for cells irradiated in G1 and G2 at 0 – 400 cGy for all four cell lines (Table 2.1). The average NDI values were 1.12 for G2 irradiated cells and 1.32 for G1 irradiated cells (data taken from Table 2.1). There were adequate numbers of scorable binucleated cells to enumerate MN and bridges throughout all the experimental conditions used in this study. There is no evidence of any dose-related response threshold from the analyses of the NDI values.

**Table 2.1. Nuclear division index data by cell line, cell cycle phase, and dose**

| Dose (cGy) | Nuclear Division Index | | | | | | | |
|---|---|---|---|---|---|---|---|---|
| | GM15510 | | GM15036 | | GM15526 | | GM15568 | |
| | G2 | G1 | G2 | G1 | G2 | G1 | G2 | G1 |
| 0 | 1.12 | 1.32 | 1.17 | 1.34 | 1.13 | 1.46 | 1.10 | 1.43 |
| 5 | 1.10 | 1.33 | 1.12 | 1.36 | 1.12 | 1.47 | 1.10 | 1.46 |
| 10 | 1.10 | 1.53 | 1.18 | 1.38 | 1.08 | 1.53 | 1.10 | 1.51 |
| 20 | 1.09 | 1.35 | 1.18 | 1.23 | 1.11 | 1.49 | 1.11 | 1.50 |
| 40 | 1.14 | 1.50 | 1.11 | 1.25 | 1.08 | 1.47 | 1.07 | 1.35 |
| 60 | 1.16 | 1.47 | 1.18 | 1.37 | 1.09 | 1.48 | 1.10 | 1.32 |
| 80 | 1.07 | 1.30 | 1.17 | 1.30 | 1.11 | 1.39 | 1.10 | 1.34 |
| 100 | 1.26 | 1.33 | 1.14 | 1.23 | 1.06 | 1.36 | 1.10 | 1.26 |
| 200 | 1.15 | 1.19 | 1.18 | 1.18 | 1.10 | 1.30 | 1.11 | 1.16 |
| 300 | 1.15 | 1.11 | 1.18 | 1.17 | 1.04 | 1.13 | 1.11 | 1.09 |
| 400 | 1.22 | 1.12 | 1.17 | 1.10 | 1.10 | 1.12 | 1.06 | 1.07 |

**Low-dose G2 slopes compared to low-dose G1 slopes**

The ratios of the low dose (0 – 20 cGy) response slopes of the cells irradiated in G2 and G1 were compared for MN (Figures 2.2, 2.3) and bridges (Figures 2.4, 2.5). Univariate regression analyses were performed individually for each cell line and replicate. As shown in Table 2.2, the slopes of the low-dose responses in G2 were at least 3.1-fold steeper for MN and 2.4-fold steeper for bridges ($p < 0.02$ in each case), than the slopes observed in G1. These results indicate that the HRS effect is clearly evident in G2 and not in G1 irradiated cells for both endpoints. Multivariate regression analyses on all cell lines considered together indicate that the slope for low doses in G2 is 6.9-fold steeper for MN ($p < 0.0001$) and 9.3-fold steeper for bridges ($p < 0.0001$) compared to the corresponding dose region in G1 (Table 2.2). Thus for all four cell lines considered together, the low-dose HRS effect is seen in G2 and not in G1.

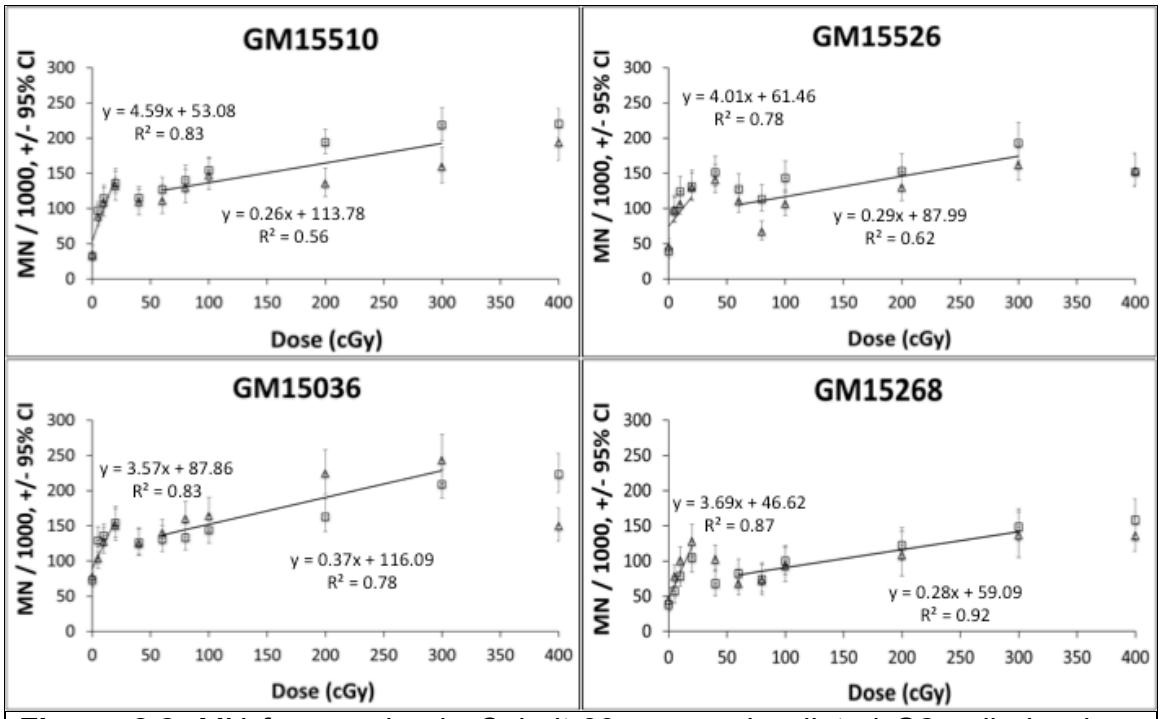


**Figure 2.2.** MN frequencies in Cobalt-60 gamma-irradiated G2 cells by dose for four human lymphoblastoid cell lines. Univariate regression analyses were performed to obtain the slopes for the low (≤ 20 cGy) and high (60 – 300 cGy) dose regions of the responses. Each panel depicts data for one cell line with replicate experiments (triangles: replicate 1; squares: replicate 2).

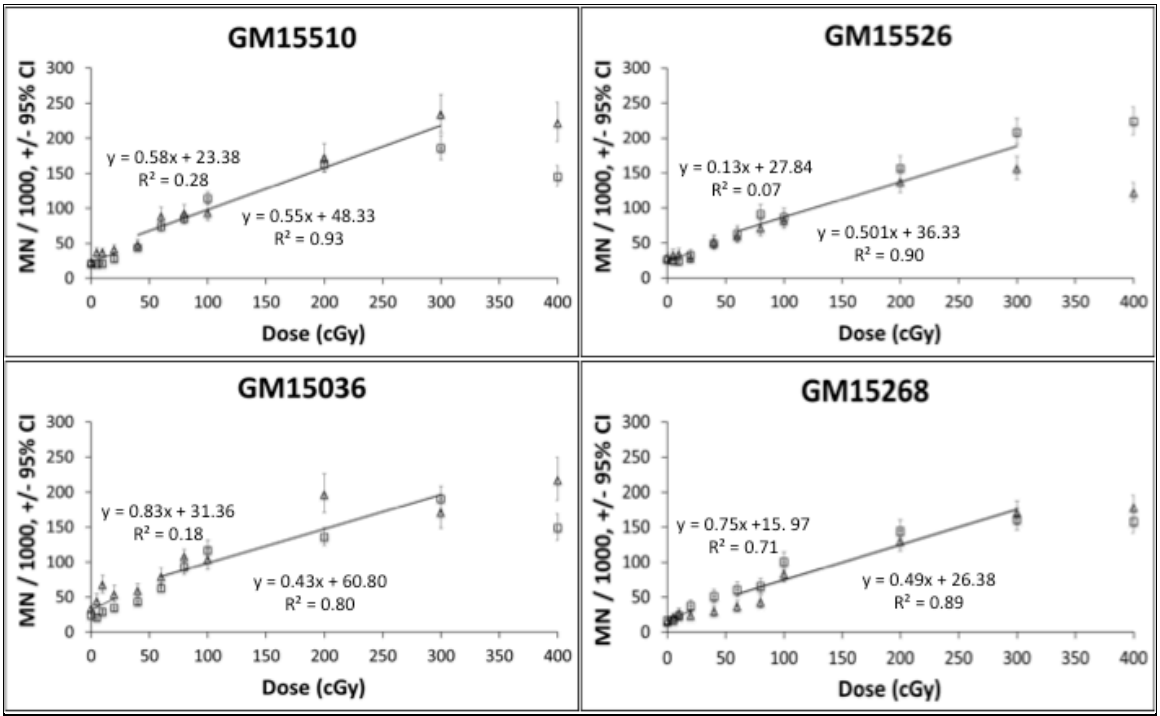


**Figure 2.3.** MN frequencies in Cobalt-60 gamma-irradiated G1 cells by dose for four human lymphoblastoid cell lines. Univariate regression analyses were performed to obtain the slopes for the low (≤ 20 cGy) and high (60 – 300 cGy) dose regions of the responses. Each panel depicts data for one cell line with replicate experiments (triangles: replicate 1; squares: replicate 2).

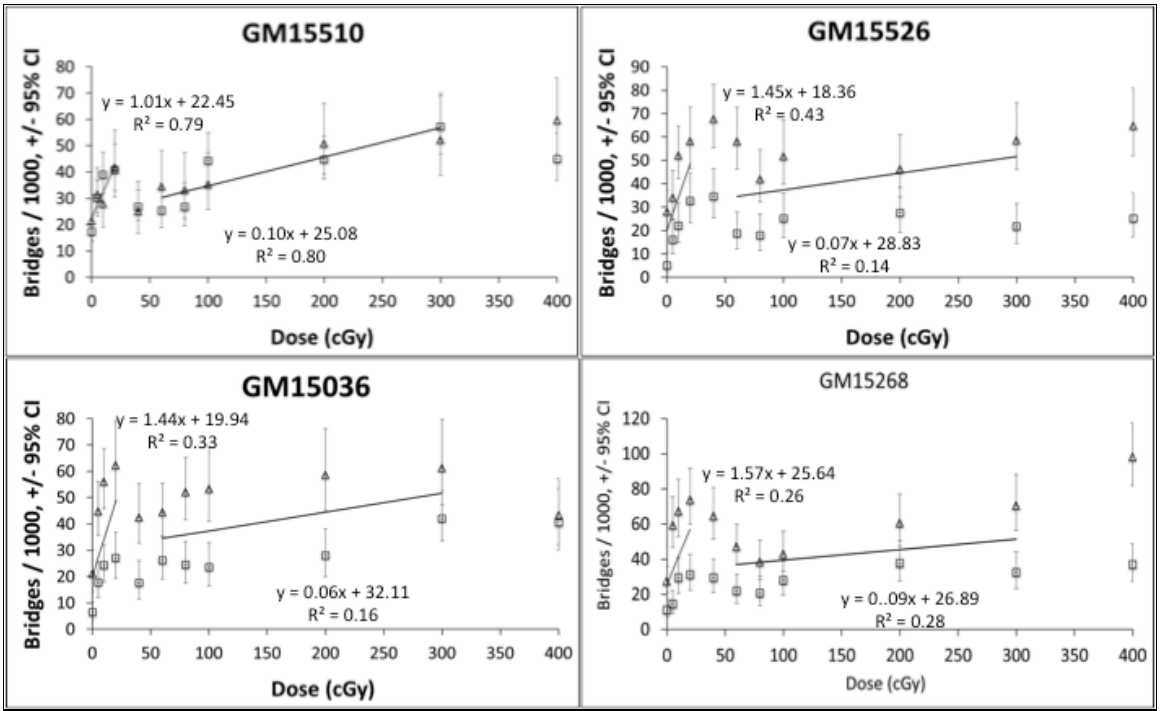


**Figure 2.4.** Bridge frequencies in Cobalt-60 gamma-irradiated G2 cells by dose for four human lymphoblastoid cell lines. Univariate regression analyses were performed to obtain the slopes for the low (≤ 20 cGy) and high (60 – 300 cGy) dose regions of the responses. Each panel depicts data for one cell line with replicate experiments (triangles: replicate 1; squares: replicate 2).

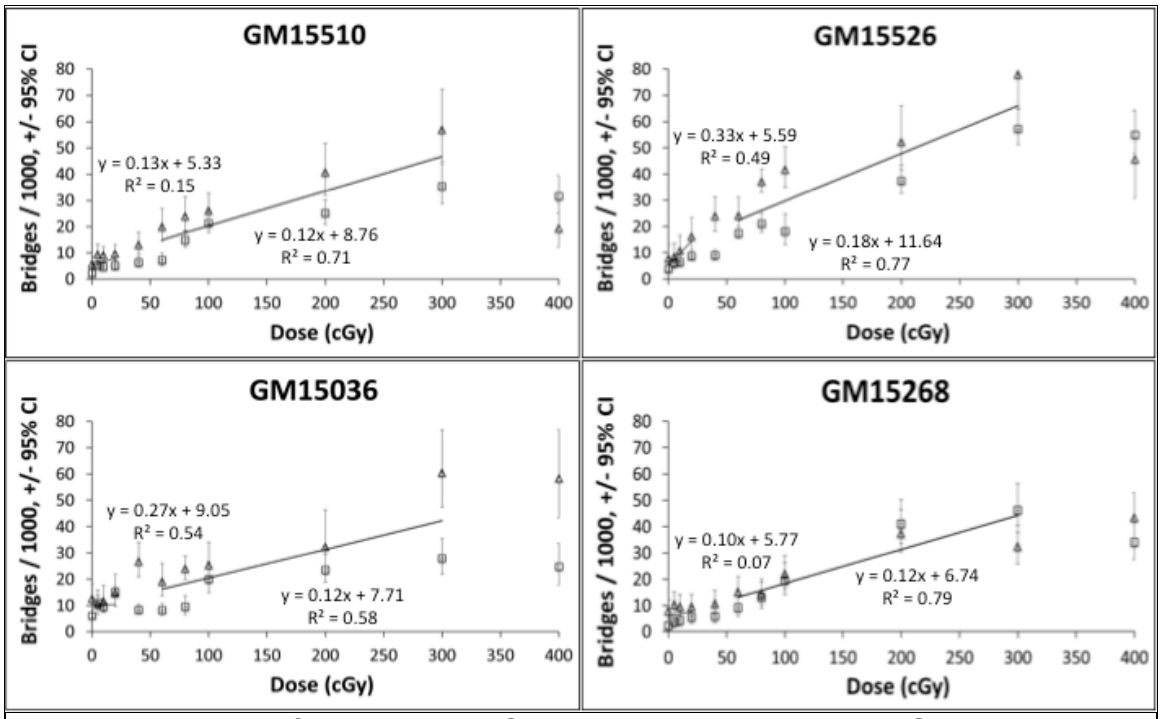


**Figure 2.5.** Bridge frequencies in Cobalt-60 gamma-irradiated G1 cells by dose for four human lymphoblastoid cell lines. Univariate regression analyses were performed to obtain the slopes for the low (≤ 20 cGy) and high (60 – 300 cGy) dose regions of the responses. Each panel depicts data for one cell line with replicate experiments (triangles: replicate 1; squares: replicate 2).

**Table 2.2. Comparisons of G2 and G1 slopes in the low dose region.**

| Cell line | Replicate | G2 | | G1 | | Ratio of slopes | p-value |
|---|---|---|---|---|---|---|---|
| | | Slope | S.E. | Slope | S.E. | | |
| Micronuclei | | | | | | | |
| All cell lines | 1 & 2 | 3.97 | 0.37 | 0.57 | 0.14 | 6.93 | < 0.0001 |
| GM15510 | 1 | 4.51 | 1.29 | 0.79 | 0.36 | 5.70 | 0.049 |
| | 2 | 4.68 | 1.64 | 0.36 | 0.14 | 12.86 | 0.058 |
| | 1 & 2 | 4.59 | 0.86 | 0.58 | 0.37 | 7.96 | 0.001 |
| GM15526 | 1 | 3.76 | 1.25 | -0.06 | 0.25 | -61.53 | 0.0401 |
| | 2 | 4.25 | 1.72 | 0.32 | 0.22 | 13.13 | 0.086 |
| | 1 & 2 | 4.01 | 0.88 | 0.13 | 0.19 | 30.51 | 0.0009 |
| GM15036 | 1 | 3.56 | 0.55 | 1.05 | 0.93 | 3.39 | 0.081 |
| | 2 | 3.58 | 1.43 | 0.61 | 0.24 | 5.82 | 0.109 |
| | 1 & 2 | 3.57 | 0.66 | 0.83 | 0.73 | 4.28 | 0.017 |
| GM15268 | 1 | 4.05 | 0.63 | 0.43 | 0.26 | 9.50 | 0.006 |
| | 2 | 3.34 | 0.29 | 1.07 | 0.18 | 3.12 | 0.002 |
| | 1 & 2 | 3.69 | 0.59 | 0.75 | 0.19 | 4.94 | 0.0004 |
| Bridges | | | | | | | |
| All cell lines | 1 & 2 | 1.37 | 0.17 | 0.15 | 0.04 | 9.32 | < 0.0001 |
| GM15510 | 1 | 0.91 | 0.28 | 0.16 | 0.10 | 5.62 | 0.06 |
| | 2 | 1.11 | 0.36 | 0.11 | 0.09 | 10.24 | 0.073 |
| | 1 & 2 | 1.01 | 0.21 | 0.13 | 0.13 | 7.47 | 0.004 |
| GM15526 | 1 | 1.58 | 0.39 | 0.45 | 0.06 | 3.53 | 0.045 |
| | 2 | 1.33 | 0.18 | 0.22 | 0.04 | 6.00 | 0.0035 |
| | 1 & 2 | 1.45 | 0.69 | 0.33 | 0.14 | 4.35 | 0.14 |
| GM15036 | 1 | 1.91 | 0.66 | 0.14 | 0.11 | 13.43 | 0.056 |
| | 2 | 0.97 | 0.33 | 0.40 | 0.13 | 2.39 | 0.018 |
| | 1 & 2 | 1.44 | 0.83 | 0.27 | 0.10 | 5.28 | 0.19 |
| GM15268 | 1 | 2.06 | 0.87 | 0.05 | 0.07 | 41.31 | 0.083 |
| | 2 | 1.09 | 0.36 | 0.15 | 0.02 | 7.03 | 0.056 |
| | 1 & 2 | 1.57 | 1.07 | 0.10 | 0.15 | 15.40 | 0.19 |

**G2 slopes, low- versus high- dose regions**

Figures 2.2 and 2.4 indicate that the slopes of the frequencies of MN and bridges, respectively, induced in G2 were much higher at low doses (0 – 20 cGy) than high doses (60 - 300 cGy). To evaluate these differences further, the ratios of the slopes of the low- and high-dose regions were calculated. Univariate linear regression analyses (Table 2.3) showed that the slopes at low doses were at least 7-fold steeper for MN and 10-fold steeper for bridges compared to the slopes at high doses when both replicates in all four cell lines were evaluated independently ($p < 0.025$ in each case). Similarly, multivariate linear regression analyses showed that the slope of the response in the low dose region is at least 13-fold and 19-fold steeper for MN and bridges, respectively ($p < 0.0001$ in each case) than at high doses (Table 2.3). Taken together, the univariate and multivariate analyses clearly indicate that the HRS effect is observed at low doses in G2 cells for both endpoints, and that the responses in G2 cells, over a broad range of doses, is not linear, i.e. the dose response for cells irradiated does not follow a LNT model.

**Table 2.3. Comparisons of G2 slopes in the low dose and the high dose regions.**

| Cell line | Replicate | Low dose | | High dose | | Ratio of slopes | p-value |
|---|---|---|---|---|---|---|---|
| | | Slope | S.E. | Slope | S.E. | | |
| Micronuclei | | | | | | | |
| All cell lines | 1 & 2 | 3.97 | 0.37 | 0.29 | 0.02 | 13.53 | < 0.0001 |
| GM15510 | 1 | 4.51 | 1.29 | 0.14 | 0.07 | 32.45 | 0.009 |
| | 2 | 4.68 | 1.64 | 0.38 | 0.04 | 12.45 | 0.011 |
| | 1 & 2 | 4.59 | 0.86 | 0.26 | 0.08 | 17.85 | 0.0006 |
| GM15526 | 1 | 3.76 | 1.25 | 0.29 | 0.10 | 12.77 | 0.048 |
| | 2 | 4.25 | 1.72 | 0.28 | 0.06 | 15.03 | 0.025 |
| | 1 & 2 | 4.01 | 0.88 | 0.29 | 0.08 | 13.88 | 0.002 |
| GM15036 | 1 | 3.56 | 0.55 | 0.43 | 0.06 | 8.25 | 0.006 |
| | 2 | 3.58 | 1.43 | 0.31 | 0.03 | 11.37 | 0.020 |
| | 1 & 2 | 3.57 | 0.66 | 0.37 | 0.07 | 9.56 | 0.0009 |
| GM15268 | 1 | 4.05 | 0.63 | 0.56 | 0.07 | 7.28 | 0.021 |
| | 2 | 3.34 | 0.29 | 0.43 | 0.08 | 7.75 | 0.009 |
| | 1 & 2 | 3.69 | 0.59 | 0.49 | 0.06 | 7.48 | 0.0005 |
| Bridges | | | | | | | |
| All cell lines | 1 & 2 | 1.37 | 0.17 | 0.07 | 0.01 | 19.16 | < 0.0001 |
| GM15510 | 1 | 0.91 | 0.28 | 0.09 | 0.02 | 10.25 | 0.025 |
| | 2 | 1.11 | 0.36 | 0.12 | 0.03 | 9.24 | 0.043 |
| | 1 & 2 | 1.01 | 0.21 | 0.10 | 0.02 | 9.67 | 0.0007 |
| GM15526 | 1 | 1.58 | 0.39 | 0.02 | 0.04 | 72.42 | 0.024 |
| | 2 | 1.33 | 0.18 | 0.02 | 0.02 | 84.17 | 0.003 |
| | 1 & 2 | 1.45 | 0.69 | 0.02 | 0.06 | 77.35 | 0.060 |
| GM15036 | 1 | 1.91 | 0.66 | 0.06 | 0.02 | 32.93 | 0.009 |
| | 2 | 0.97 | 0.33 | 0.07 | 0.02 | 14.27 | 0.025 |
| | 1 & 2 | 1.44 | 0.83 | 0.06 | 0.05 | 22.89 | 0.089 |
| GM15268 | 1 | 2.06 | 0.87 | 0.12 | 0.02 | 16.51 | 0.025 |
| | 2 | 1.09 | 0.36 | 0.05 | 0.03 | 19.94 | 0.034 |
| | 1 & 2 | 1.57 | 1.07 | 0.09 | 0.05 | 17.55 | 0.11 |

**G1 slopes, low- versus high-dose regions**

The slopes of the G1 responses at low and high doses for MN (Figure 2.3) and bridges (Figure 2.5) were then compared for all four cell lines. Univariate regression analyses revealed that the ratios of the low- to high-dose responses for both replicates in all four cell lines averaged about 1.2 for MN and 1.1 for bridges (data taken from Table 2.4). Multivariate regression analyses revealed that the ratios of the low- to high-dose slopes averaged 1.1 for MN and 1.03 for bridges; neither ratio is statistically different from 1.0 (Table 2.4). These univariate and multivariate results show that for all four cell lines, irradiation in G1 produces little or no HRS effect for either endpoint, thus LNT models for assessing radiation damage in G1 would appear to be appropriate.

**Table 2.4. Comparisons of G1 slopes in the low dose and high dose regions**.

| Cell line | Replicate | Low dose | | High dose | | Ratio of slopes | p-value |
|---|---|---|---|---|---|---|---|
| | | Slope | S.E. | Slope | S.E. | | |
| Micronuclei | | | | | | | |
| All cell lines | 1 & 2 | 0.57 | 0.14 | 0.50 | 0.03 | 1.14 | 0.62 |
| GM15510 | 1 | 0.79 | 0.36 | 0.64 | 0.04 | 1.23 | 0.78 |
| | 2 | 0.36 | 0.14 | 0.47 | 0.07 | 0.78 | 0.54 |
| | 1 & 2 | 0.58 | 0.37 | 0.55 | 0.05 | 1.04 | 0.97 |
| GM15526 | 1 | -0.06 | 0.25 | 0.42 | 0.05 | -0.15 | 0.42 |
| | 2 | 0.32 | 0.22 | 0.59 | 0.04 | 0.55 | 0.58 |
| | 1 & 2 | 0.13 | 0.19 | 0.51 | 0.06 | 0.26 | 0.54 |
| GM15036 | 1 | 1.05 | 0.93 | 0.42 | 0.15 | 2.51 | 0.73 |
| | 2 | 0.61 | 0.24 | 0.46 | 0.08 | 1.34 | 0.86 |
| | 1 & 2 | 0.83 | 0.73 | 0.44 | 0.08 | 1.90 | 0.68 |
| GM15268 | 1 | 0.43 | 0.26 | 0.56 | 0.07 | 0.77 | 0.87 |
| | 2 | 1.07 | 0.18 | 0.45 | 0.07 | 2.39 | 0.48 |
| | 1 & 2 | 0.75 | 0.19 | 0.49 | 0.06 | 1.51 | 0.68 |
| Bridges | | | | | | | |
| All cell lines | 1 & 2 | 0.15 | 0.04 | 0.14 | 0.01 | 1.03 | 0.75 |
| GM15510 | 1 | 0.16 | 0.10 | 0.15 | 0.03 | 1.07 | 0.89 |
| | 2 | 0.11 | 0.09 | 0.10 | 0.02 | 1.09 | 0.97 |
| | 1 & 2 | 0.13 | 0.13 | 0.13 | 0.03 | 1.08 | 0.97 |
| GM15526 | 1 | 0.45 | 0.06 | 0.20 | 0.03 | 2.29 | 0.014 |
| | 2 | 0.22 | 0.04 | 0.17 | 0.02 | 1.32 | 0.29 |
| | 1 & 2 | 0.33 | 0.14 | 0.18 | 0.04 | 1.84 | 0.69 |
| GM15036 | 1 | 0.14 | 0.11 | 0.16 | 0.03 | 0.91 | 0.96 |
| | 2 | 0.40 | 0.13 | 0.78 | 0.02 | 0.52 | 0.24 |
| | 1 & 2 | 0.27 | 0.10 | 0.12 | 0.04 | 2.33 | 0.68 |
| GM15268 | 1 | 0.05 | 0.07 | 0.09 | 0.03 | 0.58 | 0.67 |
| | 2 | 0.15 | 0.02 | 0.16 | 0.03 | 0.96 | 0.84 |
| | 1 & 2 | 0.10 | 0.15 | 0.12 | 0.02 | 0.82 | 0.93 |

**Radiation sensitivity per unit dose**

Figures 2.6 and 2.8 show radiation sensitivity per unit dose in G2 for MN and bridges, respectively. Radiosensitivity is clearly much more evident at doses of 20 cGy and lower than at higher doses. However, as seen in Figures 2.7 and 2.9 for MN and bridges, respectively, G1 irradiated cells show little or no radiosensitivity, indicating that G2 cells are more radiation sensitive per unit dose than G1 cells for both endpoints.

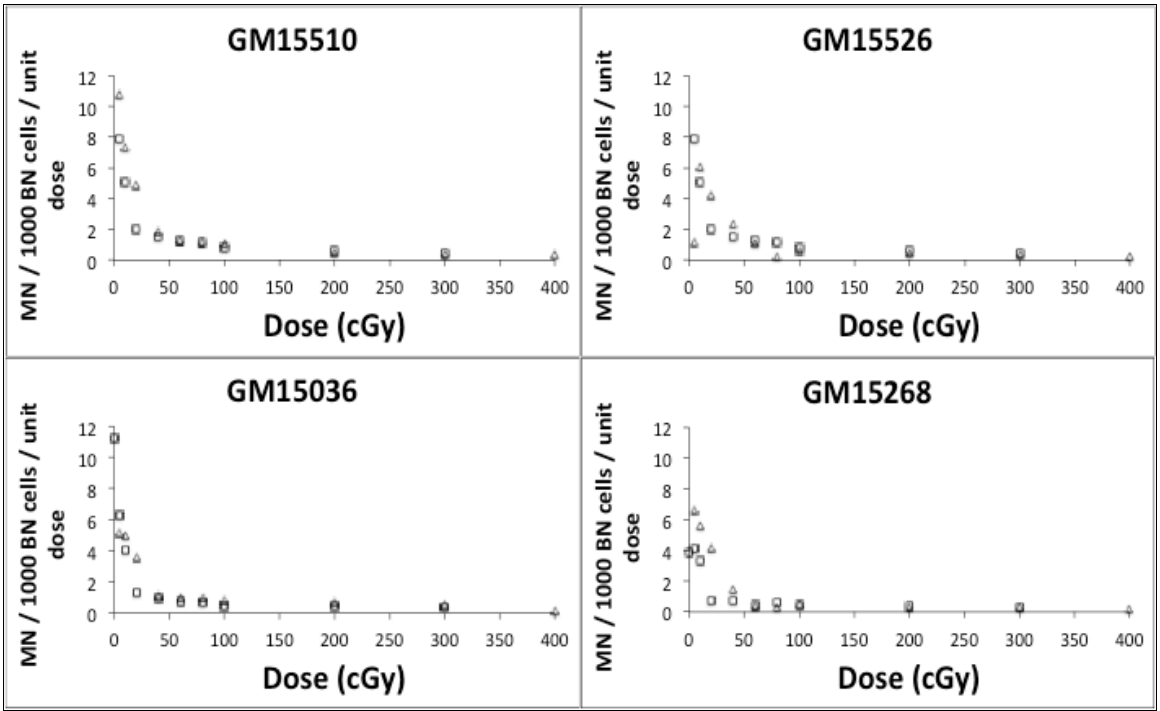


**Figure 2.6**. Radiation sensitivities for MN in Cobalt-60 gamma-irradiated G2 cells by dose for four human lymphoblastoid cell lines. The radiation sensitivities are the slopes of the line obtained between the frequency of MN at the 0 cGy dose and the frequency of MN at each individual higher dose. The G2 irradiated cells are more sensitive to radiation per unit dose for the low (≤ 20 cGy) than the high (60 – 300 cGy) dose regions. Each panel depicts data for one cell line with replicate experiments (triangles: replicate 1; squares: replicate 2).

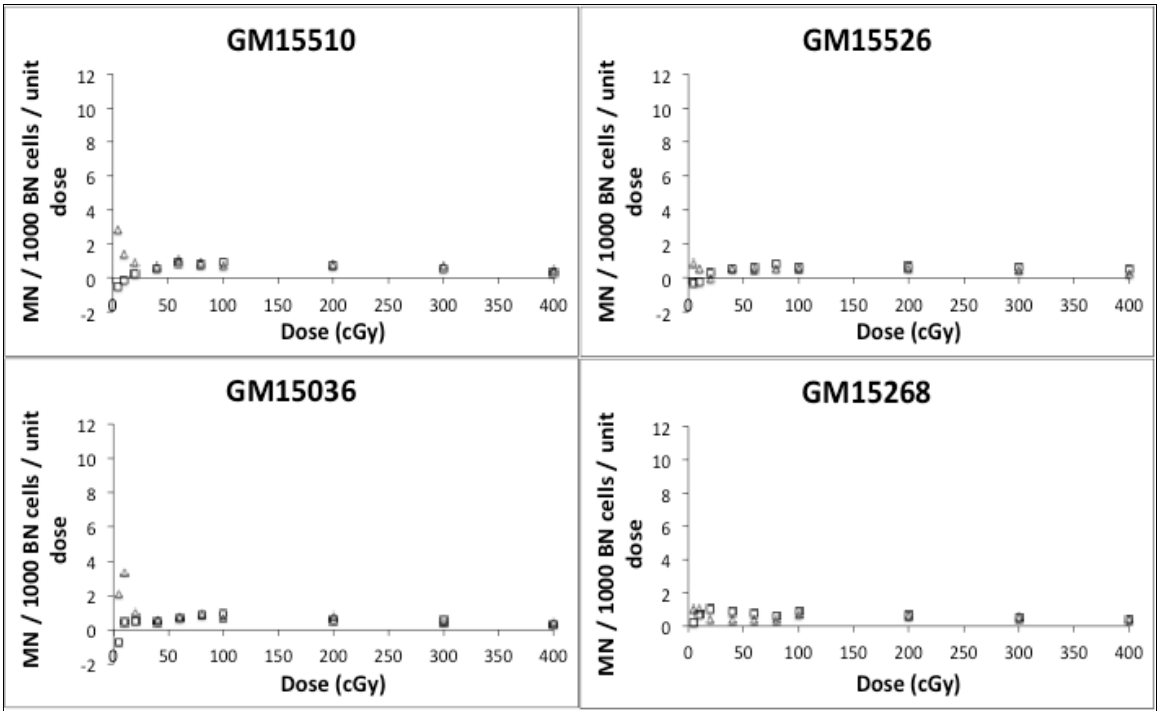


**Figure 2.7.** Radiation sensitivities of MN in Cobalt-60 gamma-irradiated G1 cells by dose for four human lymphoblastoid cell lines. The radiation sensitivities are the slopes of the line obtained between the frequency of MN at the 0 cGy dose and the frequency of MN at each individual higher dose. The G1 irradiated cells show equal sensitivity to radiation per unit dose for the entire dose range (0 – 400 cGy). The negative values at some of the very low doses are due to low numbers of events. Each panel depicts data for one cell line with replicate experiments. The scale of the vertical axes are the same here and in Figure 2.6 (triangles: replicate 1; squares: replicate 2).

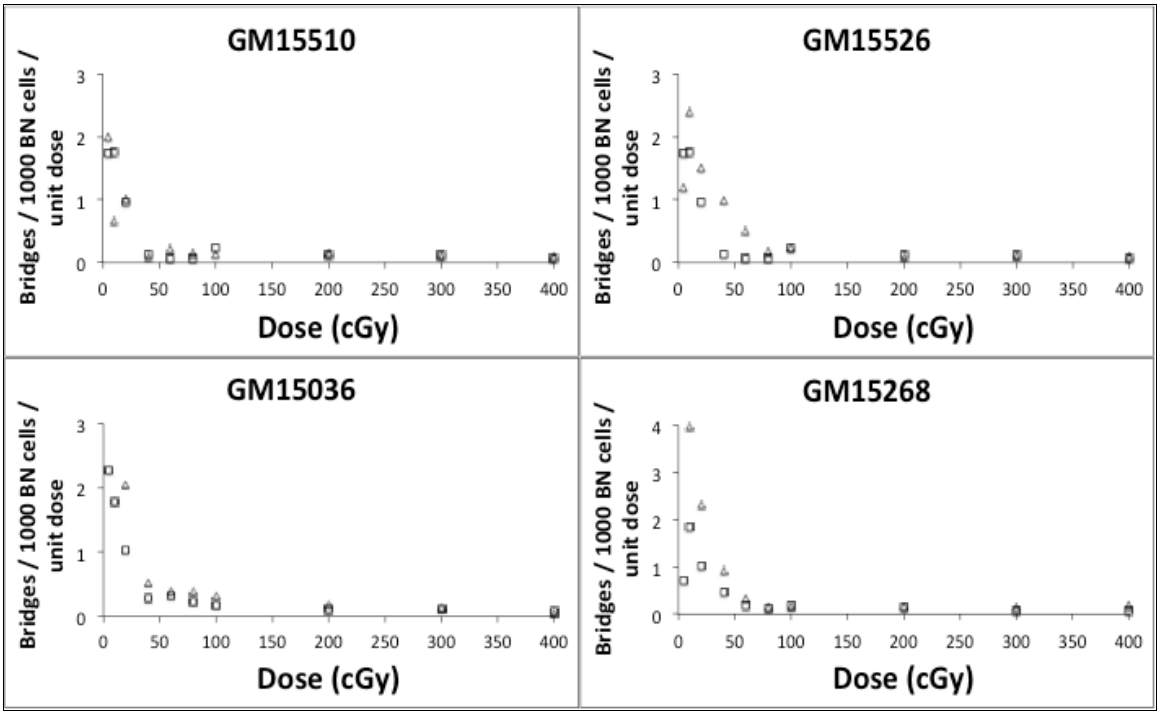


**Figure 2.8.** Radiation sensitivities of bridges in Cobalt-60 gamma-irradiated G2 cells by dose for four human lymphoblastoid cell lines. The radiation sensitivities are the slopes of the line obtained between the frequency of bridges at the 0 cGy dose and the frequency of bridges at each individual higher dose. The G2 irradiated cells are more sensitive to radiation per unit dose for the low (≤ 20 cGy) than the high (60 – 300 cGy) dose regions of the responses. Each panel depicts data for one cell line with replicate experiments (triangles: replicate 1; squares: replicate 2).

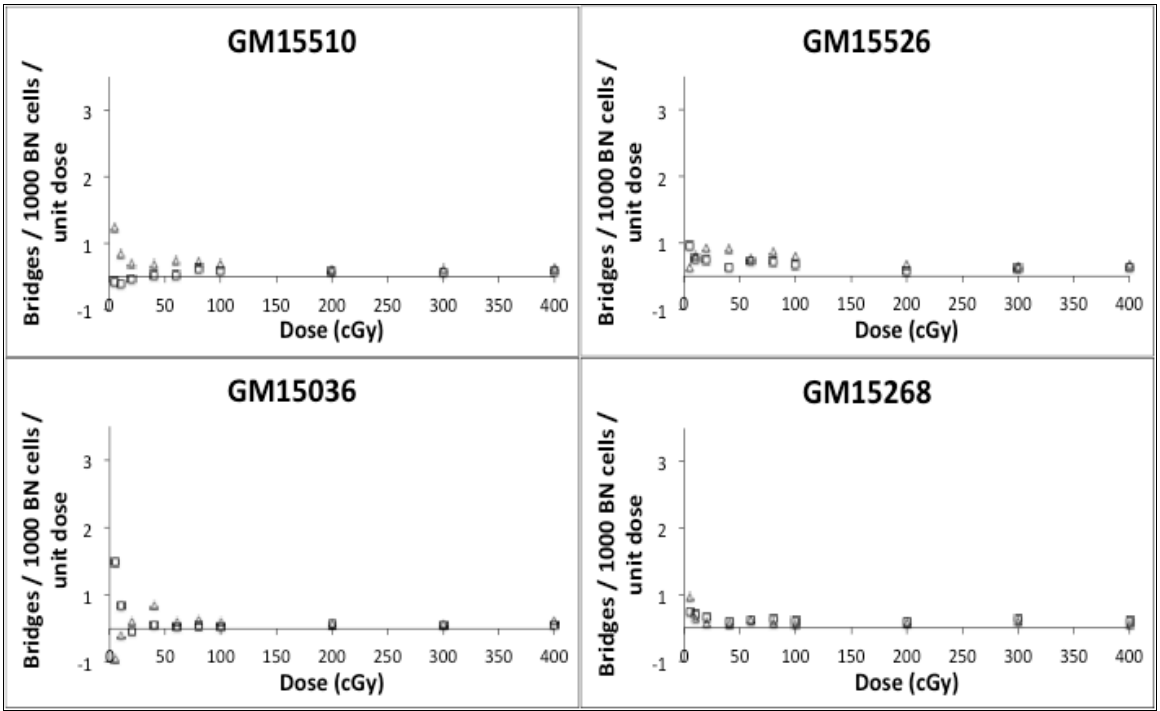


**Figure 2.9.** Radiation sensitivities of bridges in Cobalt-60 gamma-irradiated G1 cells by dose for four human lymphoblastoid cell lines. The radiation sensitivities are the slopes of the line obtained between the frequency of the bridges at the 0 cGy dose and the frequency of bridges at each individual higher dose. The G1 irradiated cells show equal sensitivity to radiation per unit dose for the entire dose range (0 – 400 cGy). The negative values at some of the very low doses are due to low numbers of events. Each panel depicts data for one cell line with replicate experiments. The scale of the vertical axes are the same here as in Figure 2.8 (triangles: replicate 1; squares: replicate 2).

## DISCUSSION

HRS has been observed in many irradiated human cell lines using clonogenic cell assays (Krueger et al. 2010). HRS may be due to inefficient activation of ATM-mediated DNA damage detection pathways at low doses that consequently fail to initiate a G2 arrest, allowing the radiation-damaged cells to enter mitosis (Wykes et al. 2006). However, the mechanism of HRS is still not completely understood. Since ionizing radiation causes DNA strand breaks, we hypothesized that the increased cell death per unit dose observed following low dose exposures should be apparent with cytogenetic endpoints.

We observed HRS in all four cell lines for doses at 20 cGy and lower as indicated by multi-fold increases in the ratio of the low-dose slopes in G2 versus G1 irradiated cells. Visual inspection of the data indicated that the low dose responses for cell lines GM15510, GM15036 and GM15268 appeared steepest from 0 - 20 cGy, and that inclusion of the 40 cGy dose would have made the low-dose regression line less steep. However, in GM15526 cells inclusion of the 40 cGy dose would not have substantially changed the slopes for either endpoint (Figures 2.2 and 2.4). For the final analyses we took a consistent statistical approach and evaluated the responses from 0 - 20 cGy for all four cell lines. However, as shown in Figures 2.6 and 2.8, the steepest slopes were for responses from 0 – 5 cGy. Had we used only these data to determine the low-dose slopes, the ratio of low- to high-dose slopes would have been higher and correspondingly more statistically significant. Thus, the approach chosen here is conservative and these ratios of low- to high-dose slopes should be considered as minimum estimates.

The observed differences in radiation sensitivities among the four cell lines may be due to genotypic differences among the people from whom these cell lines were originally established. These differences are consistent with data reported by various studies using clonogenic cell survival assays, where different cell lines exhibited an HRS effect for a range of doses ≤ 50 cGy (Marples et al. 2004; Dilworth et al. 2013; Schoenherr et al. 2013).

HRS is clearly seen in the G2 response for micronuclei and bridges. Comparison of the slopes at the low- and the high-dose regions of the dose-responses for both endpoints clearly indicate that G2 cells are more susceptible to damage per unit dose below 20 cGy than at higher doses (Figures 2.6 and 2.8). Several studies have shown that for doses below 30 cGy, cells do not appear to have efficient recognition of radiation-induced damage and thus are unable to activate the ATM-dependent G2/M checkpoint responsible for the repair, which leads to the HRS effect (Marples et al. 2003; Krueger et al. 2007b; Krueger et al. 2010). Thus, the HRS observed in this study confirms the clonogenic cell survival results and supports the idea that the lack of activation of the G2/M check point may be at least partially responsible for the increased radiosensitivity. The biphasic nature of the cytogenetic responses in irradiated G2 cells cannot be attributed to changes in the NDI since these cells exhibited little or no disruption of normal cell progression based on the NDI data (Table 2.1). The association between HRS and cytogenetic damage is clearly indicated in our study, however to take complete advantage of this effect with radiotherapy or perhaps even with chemotherapy, the mechanism of activation of the G2/M checkpoint needs to be completely elucidated, possibly in cell lines that do not show any HRS effect.

The presence of HRS in G2-irradiated cells with bridges is a novel finding. Bridges in binucleated cells are associated with dicentrics, which are formed in G1. The presence of bridges in cells that were irradiated in G2 can be attributed to chromatid exchanges ("quadriradials"), many of which will be asymmetrical, i.e., one of the four chromatids will have two centromeres. These asymmetrical chromatid exchanges will lead to bridges in binucleated cells.

The G1 responses shown here did not exhibit an HRS effect for either endpoint, suggesting that most of the radiation-induced damage to G1 cells is repaired before the cells enter mitosis. The responses of the cells irradiated in G1 for the low and high doses were comparable as indicated by the ratio of slopes (Table 2.4) for both endpoints. These results indicate that the G1 responses follow a LNT model of radiation risk assessment.

This study demonstrates an HRS effect in G2-irradiated cells for micronuclei and nucleoplasmic bridges at doses up to 20 cGy in four normal human lymphoblastoid cell lines. The results indicate that back-extrapolation of the dose response curve from high to low doses may not always provide an accurate measure of the actual DNA damage or the most optimal risk assessments. The results also suggest that individuals may differ with respect to their radiosensitivities, which may complicate estimation of individual risks of low-dose effects. Our study indicates that HRS needs to be accounted for a thorough understanding of the risks involved with low dose exposures.

# CHAPTER 3

## Effects of low oxygen levels on G2-specific cytogenetic low dose hyper-radiosensitivity in irradiated human cells

## INTRODUCTION

Cells are traditionally cultured *in vitro* with ambient atmospheric conditions where oxygen ($O_2$) levels are about 21%. In contrast, physiological $O_2$ levels are approximately 5% in normal tissue and may be lower in some solid tumor microenvironments. Compared to cells grown at physiological $O_2$ levels, culturing cells in ambient $O_2$ results in increased intracellular amounts of hydroxyl ions that result in DNA strand breaks (Henderson and Miller 1986; Boregowda et al. 2012; Koukourakis 2012). With hypoxic conditions the lower number of DNA strand breaks are repaired efficiently due to activation of ATM and ATR mediated DNA repair pathways (Cam et al. 2010; Mongiardi et al. 2011; Stagni et al. 2014). The biological effects of radiation are highly influenced by $O_2$ levels, with hypoxia and anoxia making cells two to three times more resistant to radiation (Palcic et al. 1982; Marples et al. 1994b; Hockel and Vaupel 2001; Ma et al. 2013). Tumor hypoxia, especially before radiotherapy, is known to be associated with poor clinical prognosis (Semenza 2012). Hypoxia is related to tumor development, metastatic capacity and malignant progression, and results in resistance to therapy at doses above 1 Gy (Brown et al. 2010; Hanahan and Weinberg 2011; Song et al. 2011).

Over the past few decades there has been tremendous progress in understanding the biological effects of radiation exposures ≤ 1 Gy. *In vitro* clonogenic cell survival assays have demonstrated increased death in cells irradiated below 30 cGy compared to exposures above 30 cGy, a phenomenon termed low dose hyper-radiosensitivity (HRS) (Joiner et al. 2001a; Marples and Collis 2008). HRS is

predominantly seen in cells exposed to doses ≤ 30 cGy, especially when irradiation occurs in the G2 phase of the cell cycle (Wykes et al. 2006; Martin et al. 2013). The G2-specific HRS is hypothesized to be due to inactivation of an ATM-dependent early G2/M checkpoint that causes inactivation of this DNA repair pathway, thus allowing damaged cells to enter mitosis (Xu et al. 2002; Krempler et al. 2007). We have previously observed HRS in G2-irradiated cells at exposures ≤ 20 cGy for four normal human lymphoblastoid cell lines, which were grown using standard *in vitro* cell culture techniques in ambient air (Joshi et al. 2014).

The validity of the HRS effect has been analyzed under numerous experimental conditions. The effects of dose rate (Marples and Collis 2008), priming dose (Joiner et al. 1996), $O_2$ levels of cell cultures (Marples et al. 1994a) and cell cycle phase (Short et al. 2003) have all been evaluated, and HRS has also been shown to occur *in vivo* (Marples and Collis 2008; Martin et al. 2013). In contrast, HRS was not observed in Chinese hamster cells when they were exposed to hypoxia 1 hour before irradiation (Marples et al. 1994a; Marples et al. 1994b). However, a recent study showed that HRS was transiently diminished in human breast tumor T-47D cells that were cultured for 3 – 6 weeks at 4% $O_2$ levels and that upon re-oxygenation with 20% $O_2$ the HRS effect was reestablished (Pettersen et al. 2007; Edin et al. 2012).

In the present study, we asked whether HRS occurs in cells cultured under low (2.5% and 5%) $O_2$ levels compared to cells grown in ambient air. Cells in both G1 and G2 phases were exposed to Cobalt-60 gamma radiation at doses of 0 to 400 cGy and individually characterized for cytogenetic responses using the cytokinesis-blocked micronucleus assay. For G2-irradiated cells, HRS was not observed in cells cultured at

2.5% or 5% $O_2$, but was observed at ≤ 20 cGy in cells grown in ambient air. Because elimination of HRS was observed at low $O_2$ levels, we also asked whether the loss of HRS was due to low $O_2$ conditions before and / or after radiation exposure. We therefore characterized the radiation responses of the G2 cells under two conditions: a) re-oxygenation, in which the cells were irradiated in 5% $O_2$ and then immediately transferred to ambient air, and b) hypo-oxygenation, in which the cells were irradiated in ambient air and then immediately transferred to 5% $O_2$. We observed that re-oxygenation resulted in an HRS effect at ≤ 20 cGy in both cell lines. A reverse effect was seen in hypo-oxygenated cells, wherein a pronounced reduction in HRS was observed for exposures ≤ 20 cGy. We did not observe HRS in G1-irradiated cells. However, we observed a reduction in the frequencies of MN and bridges in both G1 and G2 at 40 – 400 cGy. These results indicate that cells cultured in physiological $O_2$ levels exhibit less gamma radiation-induced cytogenetic damage than cells cultured in ambient air, indicating that ambient $O_2$ levels in tissue culture contribute to the HRS effects and exacerbate radiation sensitivities.

# MATERIALS AND METHODS

## Cell lines and cell culture

Two normal human lymphoblastoid cell lines, GM15510 and GM15036, were used in this study based on cytogenetic evidence for their HRS in our previous work (Joshi et al. 2014). Both cell lines were obtained from the Coriell Cell Repository and cultured using a protocol provided by Coriell either in ambient air (~21%) $O_2$ or at low (2.5% or 5%) $O_2$ levels. The cells were grown in T-10 flasks (Fisher Scientific, Pittsburg, PA) containing 5 ml of RPMI1640 medium (GIBCO, Grand Island, NY and Hyclone, Logan, UT) supplemented with 15% Fetal Bovine Serum (FBS, Atlanta Biologicals, Lawrenceville, GA), 2 mM L-glutamine (GIBCO, Grand Island, NY), penicillin-streptomycin (100 units/ml penicillin G Sodium, 100 µg/ml streptomycin sulfate in 0.85% saline) (GIBCO, Grand Island, NY) and fungizone (amphotericin B, 2.5 µg/ml, 0.2 mm filtered) (Hyclone, Logan, UT). Under conditions of ambient air, the flasks had loosened caps. All cultures were maintained at 37°C and 5% $CO_2$ in a fully humidified incubator, and passaged every three to four days when their density reached $10^6$ cells/ml.

## $O_2$ conditioned media (OCM)

Oxygen conditioned media was prepared by equilibration for at least 8 to 10 hours in specialized Hypoxia Chambers (Billups-Rothenberg Inc., Del Mar, CA) in the presence of an artificial atmosphere with the desired $O_2$ level (2.5% or 5%). The ambient air within these hypoxia chambers was replaced with a pre-mixed manufacturer-certified gas (Airgas, Wayne, MI) by continuous flushing at 25 liters per minute, measured using a Single Flow meter (Billups Rothenberg Inc., CA), for 4

minutes. The pre-mixed gas contained either 2.5% $O_2$, 5% $CO_2$ and 92.5% $N_2$, or 5% $O_2$, 5% $CO_2$ and 90% $N_2$. The percentage of $O_2$ in the culture media was confirmed using a dissolved oxygen meter (YSI Inc., Yellow Springs, OH).

**Cell culture at low $O_2$ levels**

Prior to irradiation, the cells were seeded at 300,000 cells/ml and grown overnight in T10 flasks (Fisher Scientific, Pittsburg, PA) containing 5 ml of OCM. The culture flasks, with fully open caps, were maintained inside fully-sealed hypoxia chambers that were initially equilibrated as described above, then additionally gassed for 4 minutes, at 25 liters per minute, every 6-8 hours both before and after irradiation to maintain the $O_2$ level. The inlet and outlet ports of the hypoxia chambers were tightly secured to prevent any gas exchange with the surrounding (ambient) air, and the chambers were then returned to the incubators and maintained at 37°.

**Irradiations**

Ten to 12 hours after seeding the flasks in OCM, the flasks were retrieved from the hypoxia chambers and the caps were immediately tightened. To maintain the intra-flask $O_2$ environment, the flasks were immediately placed in plastic Ziploc bags that were then gassed for 4 minutes, at 25 liters per minute, with 2.5% or 5% $O_2$ to flush out the ambient air. The Ziploc bags were then tightly sealed using labeling tape to maintain the $O_2$ level. This procedure avoided the potential problem of a change in the intra-flask $O_2$ levels that may result from the small amount of gas exchange that may occur through the plastic walls of the flasks. The Ziploc bags containing the flasks were then

transported in a thermal insulated container with pre-warmed packs to maintain the cells at 37°C. The cells were then acutely exposed to Cobalt-60 gamma radiation at a dose rate of approximately 27 cGy/min at the Gershenson Oncology Center, Wayne State University, Detroit, MI. Flasks from each cell line were exposed to 0, 5, 10, 20, 40, 60, 80, 100, 200, 300, or 400 cGy. For re-oxygenation and hypo-oxygenation experiments the flasks were exposed to 0, 5, 10, 20, 40, 60, 80, or 100 cGy.

**Cell cycle kinetics and harvest**

We previously used flow cytometric analysis on both cell lines cultured at ambient $O_2$ levels (Joshi et al. 2014) to measure cell cycle growth kinetics. These analyses revealed that for both cell lines, the G2 phase lasted approximately 1.5 - 2 hours and that the G1 phase was approximately 20 - 22 hours in duration. The harvest times were based on these results to ensure that most binucleated cells scored were in G2 for the HRS effect (Joiner et al. 1993) or in G1.

Because $O_2$ tension can influence cell cycle progression, the growth rates of these cells cultured at 2.5% and 5% $O_2$ were determined by a cell viability assay using 0.4% Trypan blue (in phosphate buffered saline; Fisher Scientific, Pittsburg, PA). Briefly, cells were seeded at an initial concentration of approximately 300,000 cells per ml and cultured at set $O_2$ levels (2.5%, 5% and ambient air) in hypoxia chambers as described above. An aliquot of cells was taken every 24 hours. Trypan blue was added to this aliquot in a 1:1 ratio and the number of live cells per ml was determined using a standard hemocytometer (Fisher Scientific, Pittsburg, PA). The flasks were immediately returned to the hypoxia chambers and gassed for 2 minutes every 6 - 8 hours as

described above. The growth kinetics of both cell lines at 2.5 % and 5% $O_2$ were comparable to those at ambient air, thus the harvest times were established as 2 and 22 hours after radiation for the G2 and G1 phases, respectively.

**Re-oxygenation – cell culture**

Both cell lines were cultured overnight in OCM maintained at 5% $O_2$ levels in hypoxia chambers as described above. Prior to irradiation, the flasks were removed from the hypoxia chambers, the caps were immediately tightened and placed in Ziploc bags that were then flushed with premixed gas containing 5% $O_2$, 5% $CO_2$ and 90% $N_2$ to replace the ambient air and then irradiated as described above. Post-irradiation, the cells were transferred from the culture flasks into 15 ml Falcon centrifuge tubes then immediately pelleted by centrifugation at 1400 g for 5 minutes. Each cell pellet was immediately re-oxygenated by transferring it to 5 ml of pre-warmed media maintained at ambient $O_2$ levels in T10 culture flasks which were then returned to the fully humidified incubators (i.e. not in hypoxia chambers) maintained at 37°C with 5% $CO_2$ for 2 hours for G2, or 22 hours for G1, as described above.

Since re-oxygenation involved pelleting the cells by centrifugation, we included controls to rule out the possibility that this additional manipulation might influence the results. For these centrifuge controls, cells were cultured and irradiated at ambient air, then transferred to T-10 flasks containing pre-warmed media maintained at ambient air. The flasks were then returned to a fully humidified incubator and maintained at 37°C with 5% $CO_2$ for 2 hours for G2, or 22 hours for G1, as described above.

**Hypo-oxygenation – cell culture**

Both cell lines were cultured and irradiated at ambient $O_2$ levels at 37°C with 5% $CO_2$ overnight as described above. Post irradiation, these cells were transferred from the culture flasks into 15 ml Falcon tubes then immediately pelleted at 1400 g for 5 minutes. The cell pellets were immediately hypo-oxygenated by transferring them to T10 culture flasks containing 5 ml of pre-warmed OCM maintained at 5% $O_2$ levels. The flasks were then placed in hypoxia chambers and gassed with 5% $O_2$ as described above and immediately returned to the 37°C incubator for 2 hours for G2 and 22 hours for G1. Centrifuge controls were included in the experiment as described above for both cell lines.

**Cytokinesis-blocked micronucleus (CBMN) assay**

Cytogenetic damage was measured using the CBMN assay (Fenech 2000; Cheong et al. 2013). Immediately post-irradiation, 6 μg/ml of Cytochalasin B (final concentration; Sigma Aldrich, St. Louis, MO) was added to each flask. All flasks were returned to the hypoxia chambers maintained at their set $O_2$ levels, then returned to the incubator for 2 or 22 hours depending on the harvest time. The flasks were then removed from the hypoxia chambers and the caps were immediately tightened to avoid gas exchange with ambient air. The cells were resuspended and spun onto pre-cleaned microscope slides using a cytocentrifuge (Statspin, Westwood, MA) at 1300 g for 4 minutes and then air-dried. The cells were fixed in 100% methanol (Fisher Scientific, Pittsburgh, PA) for 15 minutes and stained with 10% Giemsa (Sigma Aldrich, St. Louis, MO) dissolved in water for 15 minutes, then briefly rinsed in water and air-dried.

**Data collection**

Slide readers were extensively trained prior to data collection. Equivalent numbers of cells were scored by an equal number of readers for each treatment condition, for both cell lines and both harvest times. To ensure that adequate numbers of binucleated cells were available after irradiation for all $O_2$ levels, the nuclear division index (NDI) was calculated as described (Eastmond and Tucker 1989a). Briefly, for each treatment condition a total number of 200 cells were counted to determine the frequency of cells with 1, 2, 3 or 4 nuclei using the formula

$$NDI = (M_1 + 2M_2 + 3M_3 + 4M_4) / N$$

where $M_1$ to $M_4$ represent the number of cells with 1 to 4 nuclei and N is the total number of cells scored.

**Cell scoring criteria**

Based on established criteria, the slides were evaluated for micronuclei, nucleoplasmic bridges, and buds simultaneously (Fenech 2000; Cheong et al. 2013) using Nikon Eclipse E200 light microscopes at 1000X magnification. Briefly, only binucleated cells with intact cell membranes were scored where the two main nuclei were separate from each other. Micronuclei were required to be one-third the size of the main nuclei or smaller. Each micronucleus had to be located within the cytoplasm, stained similar to the main nuclei with smooth edges, and shaped round or oval. Nucleoplasmic bridges were required to be stained similar to and connected with both the main nuclei. Buds were also scored but they did not yield meaningful results and therefore, these data are not reported here. To avoid observer bias all slides were

coded prior to scoring. For each treatment condition, at least 1000 binucleated cells were scored.

**Statistical analyses**

The cytogenetic damage data were regressed against dose to characterize HRS effects by evaluating the slopes of the responses of the G1- and G2-irradiated cells. Multivariate analyses were performed separately for three different dose ranges: 0 – 20 cGy, 40 – 100 cGy, and 200 – 400 cGy. Within each dose range the effects of $O_2$ were evaluated based on a nominal categorization of the six $O_2$ treatment levels, i.e. 2.5% $O_2$, 5% $O_2$, centrifuge controls, ambient air, post-exposure hypo-oxygenation, and post-exposure re-oxygenation. The frequencies of MN and bridges per 1000 binucleated cells were regressed against terms for dose, cell line, $O_2$ treatment group, and all the corresponding interaction terms. All analyses were performed separately for cells irradiated in G1 and G2. Tukey's HSD test was used to make post-hoc comparisons. All analyses were performed using JMP software, version 6.0, SAS Institute Inc. The 95% confidence intervals were calculated as previously described (Lilienfeld et al. 1967).

## RESULTS

The effects of atmospheric $O_2$ levels during cell culture on the frequencies of MN and nucleoplasmic bridges were assessed in cytokinesis-blocked binucleated normal human lymphoblastoid cells irradiated with Cobalt-60 gamma rays over a wide range of doses in G1 and G2 phases of the cell cycle. Table 3.1 shows the cytogenetic consequences of culturing and irradiating cells in 2.5% and 5% $O_2$ compared to cells grown and irradiated in ambient air at low doses (0 - 20 cGy) (Figures 1 and 2). For MN the ratios of the response slopes of cells cultured and irradiated in ambient air at 0 - 20 cGy were 9.6- and 7.3-fold higher at 2.5% and 5% $O_2$, respectively for GM15510 cells, and 3.2- and 5.5-fold higher, respectively for GM15036 cells. These ratios indicate the presence of HRS when these cells are cultured in ambient air, and that HRS is lost at 2.5% and 5% $O_2$. For bridges, the low-dose slopes did not show consistent trends for either cell line at 2.5% or 5% $O_2$. Since we observed low dose HRS at 5% $O_2$, which approximates the physiological $O_2$ concentration in most human tissues, we further studied the effects of re-oxygenating cells to ambient $O_2$ levels immediately after irradiating them in 5% $O_2$ (Figures 3 and 4). For both MN and bridges the dose responses for cells maintained entirely in ambient air and irradiated in G2 were very similar to the responses for cells that were cultured and irradiated in 5% $O_2$ and then immediately re-oxygenated to ambient air levels at doses of 0 – 20 cGy (Table 3.1). These results indicate that the HRS response is restored when cells are cultured in ambient $O_2$ levels post-irradiation. We also evaluated the consequences of hypo-oxygenation, i.e. cells that had been

**Table 3.1. Comparison of slopes at 0 – 20 cGy at different $O_2$ levels for cells irradiated in G2.**

| $O_2$ levels | Cell line | Slope | S.E. | Slope | S.E. | Ratio of slopes |
|---|---|---|---|---|---|---|
| Micronuclei | | | | | | |
| GM15510 | Ambient air | 4.51 | 1.29 | | | |
| | Centrifuge | | | 3.63 | 1.13 | 1.24 |
| | 2.5% | | | 0.47 | 0.07 | 9.62 |
| | 5% | | | 0.62 | 0.15 | 7.28 |
| | Re-oxygenation | | | 3.71 | 0.43 | 1.22 |
| | Hypo-oxygenation | | | 0.94 | 0.71 | 4.81 |
| GM15036 | Ambient air | 3.56 | 0.55 | | | |
| | Centrifuge | | | 3.95 | 1.27 | 0.90 |
| | 2.5% | | | 1.11 | 0.38 | 3.21 |
| | 5% | | | 0.65 | 0.33 | 5.49 |
| | Re-oxygenation | | | 4.46 | 1.87 | 0.80 |
| | Hypo-oxygenation | | | 0.19 | 0.67 | 18.33 |
| Bridges | | | | | | |
| GM15510 | Ambient air | 0.91 | 0.28 | | | |
| | Centrifuge | | | 1.49 | 0.63 | 0.61 |
| | 2.5% | | | 0.18 | 0.24 | 5.08 |
| | 5% | | | -0.15 | 0.39 | -5.98 |
| | Re-oxygenation | | | 1.23 | 0.32 | 0.74 |
| | Hypo-oxygenation | | | 0.30 | 0.16 | 3.06 |
| GM15036 | Ambient air | 1.91 | 0.66 | | | |
| | Centrifuge | | | 1.42 | 0.68 | 1.35 |
| | 2.5% | | | -0.71 | 0.39 | -2.69 |
| | 5% | | | 0.18 | 0.51 | 10.91 |
| | Re-oxygenation | | | 1.55 | 0.63 | 1.24 |
| | Hypo-oxygenation | | | 0.26 | 0.18 | 7.28 |

a: the ratio is obtained by comparing the slope at ambient air with other $O_2$ slopes individually

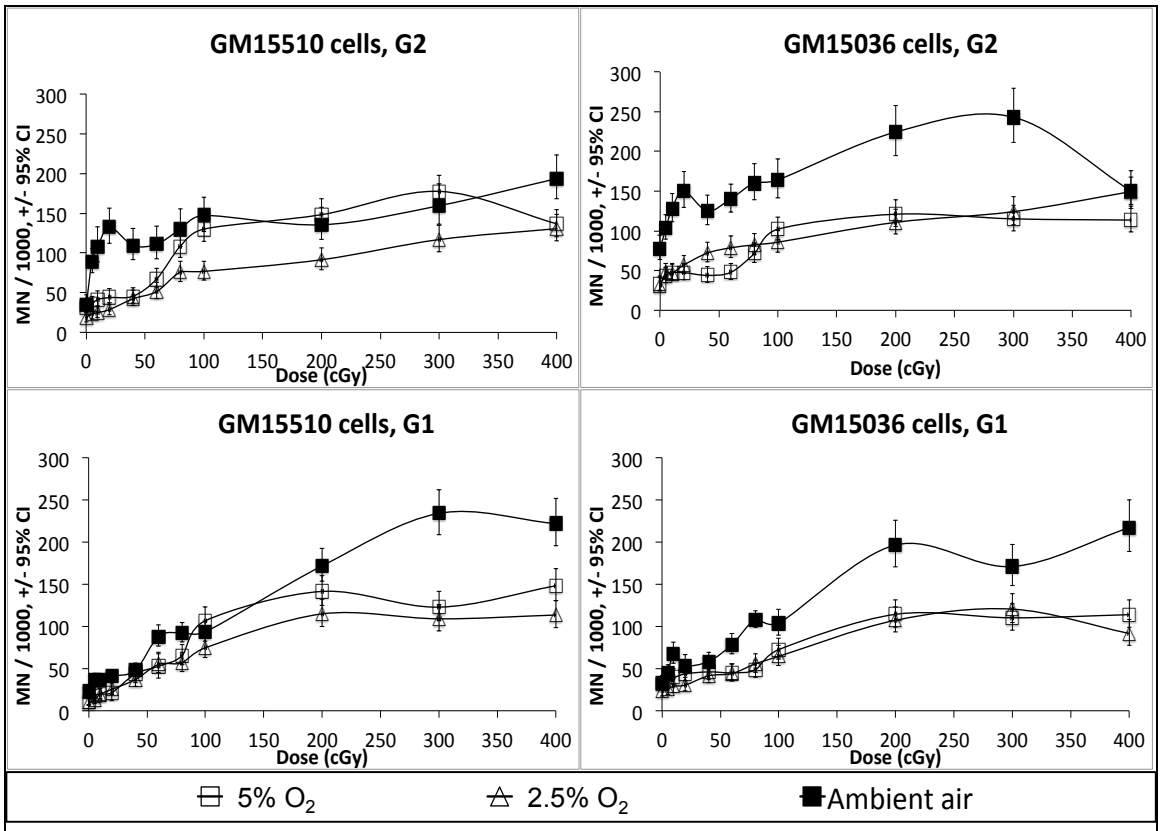


**Figure 3.1.** MN frequencies at different $O_2$ levels in two human lymphoblastoid cell lines exposed to Cobalt-60 gamma rays in G2 or G1. In G2 cells irradiated in ambient air a clear local maximum is observed at 20 cGy for both cell lines, but no such effect is seen for cells irradiated in 2.5% or 5% $O_2$. For G2-irradiated GM15036 cells, MN frequencies are much reduced for 0 – 300 cGy in 2.5% and 5% $O_2$. The responses of the G1 cells irradiated at 100 cGy and below are similar for all $O_2$ levels, however at doses of 200 - 400 cGy the MN frequencies are considerably lower for both cell lines. The 0 – 100 cGy data appear in an expanded format in Fig. 3, along with additional data.

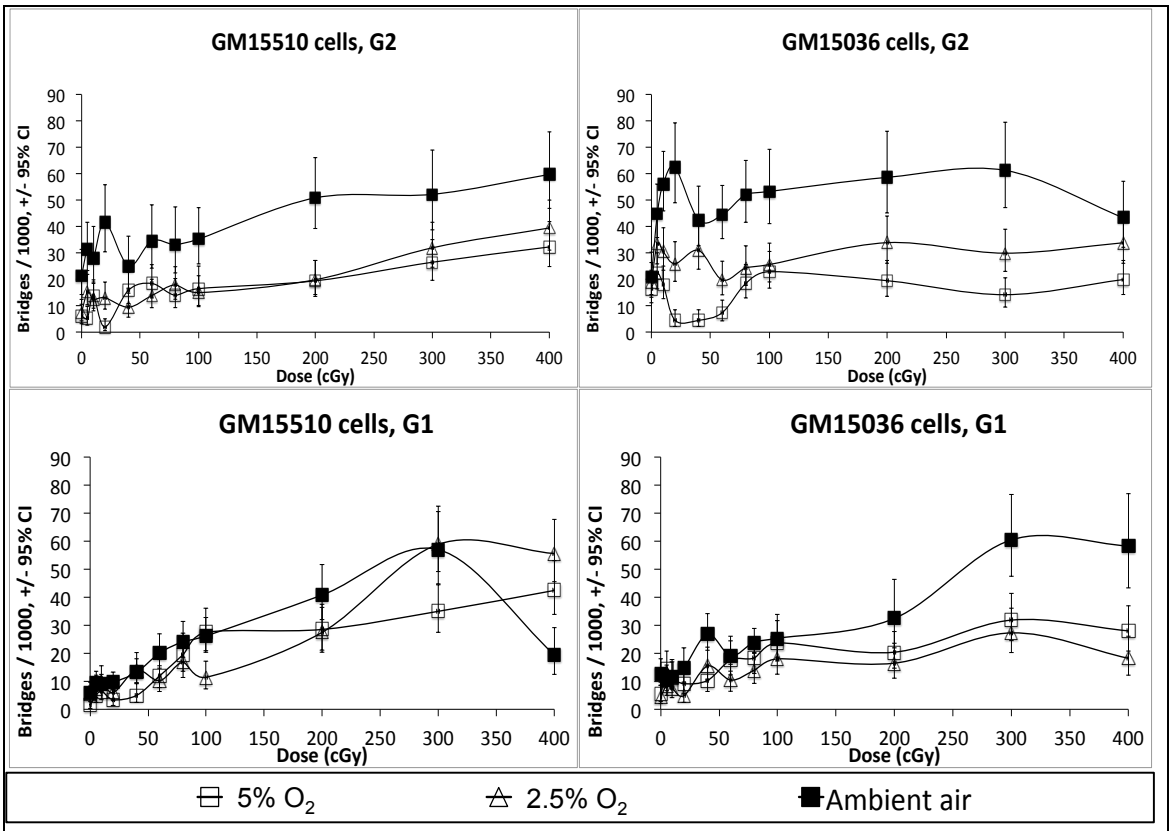


**Figure 3.2.** Frequencies of nucleoplasmic bridges at different $O_2$ levels in two human lymphoblastoid cell lines exposed to Cobalt-60 gamma rays in G2 and G1. In G2 cells irradiated in ambient air a clear local maximum is observed at 20 cGy for both cell lines, but no such effect is seen for cells irradiated in 2.5% or 5% $O_2$. Overall at doses of 0 – 300 cGy, the frequencies of bridges are much reduced in 2.5% and 5% $O_2$ for both cell lines. The responses of the G1 cells irradiated at 20 cGy and below are similar for all $O_2$ levels, however, at doses of 40 – 100 cGy the frequencies of bridges appear to be similar. At 200 – 300 cGy the frequency of bridges is much reduced in 2.5% and 5% $O_2$ in G1 for both cell lines. The 0 – 100 cGy data also appear in Fig. 4, along with additional data.

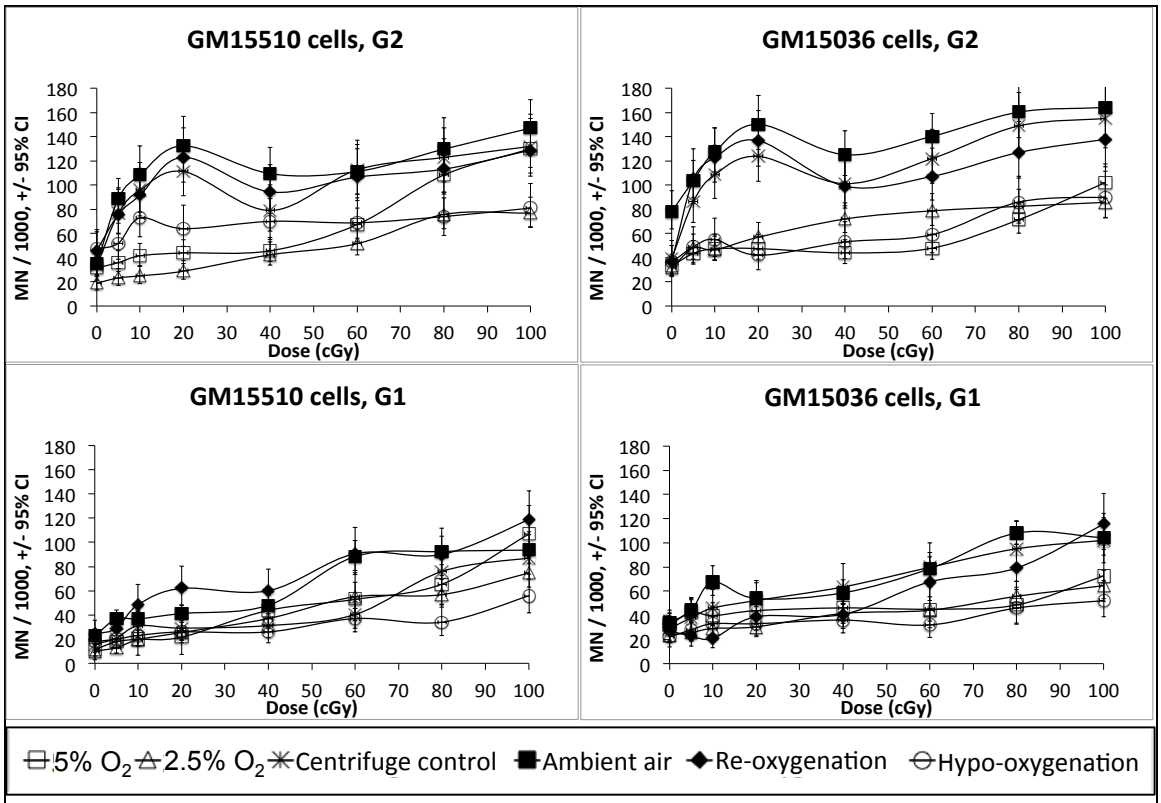


**Figure 3.3.** MN frequencies among normal human lymphoblastoid cells cultured in different $O_2$ treatment levels and exposed to Cobalt-60 gamma rays in G2 or G1. In G2 cells cultured in ambient $O_2$ following irradiation there is a clear local maximum response at 20 cGy. Cells cultured in atmospheres of 5% $O_2$ or less following irradiation showed little to no such local maximum, indicating the absence of HRS at low $O_2$ levels. At doses of 40 – 100 cGy, for G2-irradiated cells, the MN frequencies are lower at low $O_2$ levels. The dose responses of the G1-irradiated cells are much more similar to each other than the G2-irradiated cells at all doses for all $O_2$ treatment levels. The 2.5%, 5%, and ambient air data also shown in Fig. 1 at doses ≤ 100 cGy.

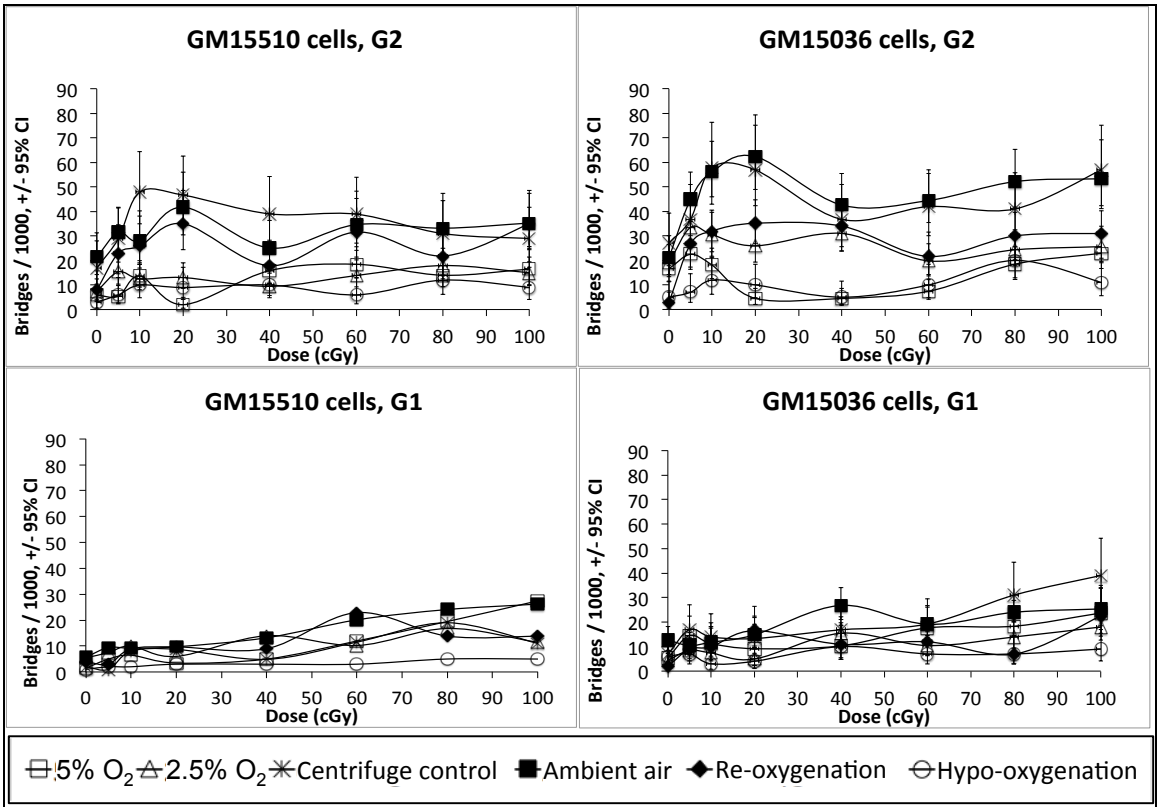


**Figure 3.4.** Frequencies of nucleoplasmic bridges among normal human lymphoblastoid cells cultured in different $O_2$ treatment levels and exposed to Cobalt-60 gamma rays in G2 or G1. In G2 cells cultured in ambient $O_2$ following irradiation there is a clear local maximum response at 20 cGy. Cells cultured in atmospheres of 5% $O_2$ or less following irradiation showed little to no such local maximum, indicating the absence of HRS at low $O_2$ levels. At doses of 40 – 100 cGy, for G2-irradiated cells, the frequencies of bridges appear to be lower at low $O_2$ levels post-irradiation. The dose responses of the G1-irradiated cells are much more similar to each other than the G2-irradiated cells at all doses for all $O_2$ treatment levels. The 2.5%, 5%, and ambient air data are also shown in Fig. 2 for doses ≤ 100 cGy.

cultured and irradiated in ambient air and then were immediately transferred after irradiation to conditioned culture medium and an atmosphere of 5% $O_2$ (Figures 3 and 4). The ratios of the low dose slopes for cells irradiated in G2 in ambient air were at least 4.8- and 3-fold steeper for MN and bridges, respectively, compared to post-irradiation hypo-oxygenated cells (Table 3.1), indicating that upon hypo-oxygenation the HRS effect is reduced compared to cells grown in ambient air.

We also studied the cytogenetic effects of low $O_2$, post-irradiation re-oxygenation and hypo-oxygenation in the G1 phase. The average of the response slopes at 0 – 20 cGy in both cell lines grown in 2.5% and 5% $O_2$, and post-irradiation hypo-oxygenation, was approximately 1.9 for MN and 0.11 for bridges (data taken from Table 3.2). Furthermore, the response slopes of post-irradiation re-oxygenated cells were no greater than 1.63 for MN and 0.48 for bridges compared to cells maintained and irradiated in ambient air. None of the ratios of slopes for any of the $O_2$ treatment levels compared to ambient air shown in Table 3.2 are statistically significant for either MN or bridges, indicating that the HRS effects were not seen in these cells in G1 at the $O_2$ levels used in this study.

Table 3.3 shows the low dose (0 – 20 cGy) response slopes of cells irradiated in G2 compared to the low dose response slopes for cells irradiated in G1 for each $O_2$ level and cell line for both MN and bridges. For MN, the slopes in G2 at ambient $O_2$ levels were at least 3.39-fold steeper than the G1 slopes, indicating a G2-specific HRS effect in ambient air. However at low $O_2$ levels, the ratios of the slopes for both cell lines averaged 1.63 for MN (data taken from Table 3.3), indicating that G2-irradiated cells are more prone to cytogenetic

**Table 3.2. Comparison of slopes at 0 -20 cGy at different $O_2$ levels for cells irradiated in G1.**

| $O_2$ levels | Cell line | Slope | S.E. | Slope | S.E. | Ratio of slopes[a] |
|---|---|---|---|---|---|---|
| Micronuclei | | | | | | |
| GM15510 | Ambient air | 0.79 | 0.36 | | | |
| | Centrifuge | | | 0.69 | 0.34 | 1.14 |
| | 2.5% | | | 0.80 | 0.09 | 0.98 |
| | 5% | | | 0.46 | 0.17 | 1.72 |
| | Re-oxygenation | | | 2.01 | 0.33 | 0.39 |
| | Hypo-oxygenation | | | 0.41 | 0.04 | 1.95 |
| GM15036 | Ambient air | 1.05 | 0.93 | | | |
| | Centrifuge | | | 1.14 | 0.22 | 0.93 |
| | 2.5% | | | 0.34 | 0.08 | 3.08 |
| | 5% | | | 0.48 | 0.29 | 2.19 |
| | Re-oxygenation | | | 0.65 | 0.48 | 1.63 |
| | Hypo-oxygenation | | | 0.53 | 0.22 | 2.00 |
| Bridges | | | | | | |
| GM15510 | Ambient air | 0.16 | 0.10 | | | |
| | Centrifuge | | | 0.40 | 0.17 | 0.40 |
| | 2.5% | | | 0.24 | 0.02 | 0.67 |
| | 5% | | | 0.07 | 0.17 | 2.35 |
| | Re-oxygenation | | | 0.34 | 0.15 | 0.48 |
| | Hypo-oxygenation | | | 0.09 | 0.16 | 1.77 |
| GM15036 | Ambient air | 0.14 | 0.11 | | | |
| | Centrifuge | | | 0.19 | 0.32 | 0.74 |
| | 2.5% | | | -0.03 | 0.16 | -5.20 |
| | 5% | | | 0.07 | 0.31 | 2.10 |
| | Re-oxygenation | | | 0.67 | 0.13 | 0.21 |
| | Hypo-oxygenation | | | -0.14 | 0.12 | -1.04 |

a: the ratio is obtained by comparing the slope at ambient air with other $O_2$ slopes individually.

**Table 3.3. Comparison of G1 and G2 slopes at different $O_2$ levels.**

| $O_2$ levels | Cell line | G2 | | G1 | | Ratio of slopes |
|---|---|---|---|---|---|---|
| | | Slope | S.E. | Slope | S.E. | |
| Micronuclei | | | | | | |
| Ambient air | GM15510 | 4.51 | 1.29 | 0.79 | 0.36 | 5.70 |
| | GM15036 | 3.56 | 0.55 | 1.05 | 0.93 | 3.39 |
| Centrifuge | GM15510 | 3.63 | 1.13 | 0.69 | 0.34 | 5.25 |
| | GM15036 | 3.95 | 1.27 | 1.14 | 0.22 | 3.47 |
| 2.5% | GM15510 | 0.47 | 0.07 | 0.80 | 0.09 | 0.58 |
| | GM15036 | 1.11 | 0.38 | 0.34 | 0.08 | 3.25 |
| 5% | GM15510 | 0.62 | 0.15 | 0.46 | 0.17 | 1.35 |
| | GM15036 | 0.65 | 0.33 | 0.48 | 0.29 | 1.35 |
| Re-oxygenation | GM15510 | 3.71 | 0.43 | 2.01 | 0.33 | 1.85 |
| | GM15036 | 4.46 | 1.87 | 0.65 | 0.48 | 6.89 |
| Hypo-oxygenation | GM15510 | 0.94 | 0.71 | 0.41 | 0.04 | 2.31 |
| | GM15036 | 0.19 | 0.67 | 0.53 | 0.22 | 0.37 |
| Bridges | | | | | | |
| Ambient air | GM15510 | 0.91 | 0.28 | 0.16 | 0.10 | 5.62 |
| | GM15036 | 1.91 | 0.66 | 0.14 | 0.12 | 13.43 |
| Centrifuge | GM15510 | 1.50 | 0.63 | 0.40 | 0.17 | 3.75 |
| | GM15036 | 1.55 | 0.63 | 0.19 | 0.32 | 8.04 |
| 2.5% | GM15510 | 0.18 | 0.24 | 0.02 | 0.17 | 9.28 |
| | GM15036 | 0.18 | 0.51 | -0.03 | 0.16 | -6.40 |
| 5% | GM15510 | -0.15 | 0.39 | 0.07 | 0.17 | -2.21 |
| | GM15036 | -0.71 | 0.39 | 0.07 | 0.31 | -10.47 |
| Re-oxygenation | GM15510 | 1.23 | 0.32 | 0.34 | 0.15 | 3.66 |
| | GM15036 | 1.42 | 0.68 | 0.67 | 0.13 | 2.12 |
| Hypo-oxygenation | GM15510 | 0.30 | 0.16 | 0.09 | 0.02 | 3.25 |
| | GM15036 | 0.26 | 0.18 | -0.14 | 0.12 | -1.92 |

damage at 2.5% and 5% $O_2$ compared to the G1 irradiated cells. For bridges the average ratio of the slopes was negative, indicating there is no HRS effect for this endpoint at 2.5% or 5% $O_2$. The average slope values for MN or bridges indicate that cells irradiated in G2 do not exhibit an HRS effect when grown in low levels of $O_2$. Moreover, as indicated in Table 3.3, for cells irradiated in G2, re-oxygenation led to slopes that were at least 1.8-fold steeper for MN and 2.1-fold steeper for bridges than the slopes for cells irradiated in G1, indicating an HRS effect after increasing the post-irradiation $O_2$ to the ambient level. However, as indicated in Table 3.3, hypo-oxygenation for cells irradiated in G2 did not consistently exhibit HRS for MN or bridges (Table 3.3).

Multivariate linear regression analyses were performed to evaluate the effects of $O_2$ concentrations on the G2 and G1 responses for each of the three dose groups, i.e., 0 – 20 cGy, 40 – 100 cGy, and 200 – 400 cGy (Tables 3.4, 3.5, and 3.6, respectively). For the dose groups 0 – 20 cGy and 40 – 100 cGy, a statistically significant $O_2$ effect independent of the dose and cell line for both MN and bridges ($p < 0.0001$ in most cases) was observed in G2 and G1 (Tables 3.4 and 3.5). However for doses of 200 – 400 cGy, a statistically significant $O_2$ effect was observed both in G2 ($p < 0.006$) and G1 ($p < 0.0004$) for MN, whereas for bridges, a significant $O_2$ effect was only seen in G2 ($p < 0.0001$) and not in G1 (Table 3.6). None of the other factors were significant for either endpoint in the highest dose group. Overall, these results indicate that at low $O_2$ levels the observed loss of HRS in G2-irradiated cells seen in Figures 1 and 2 is statistically significant.

**Table 3.4. Multivariate analyses of 0 - 20 cGy dose responses in G2 and G1**

| Source | df | G2 | | | G1 | | |
|---|---|---|---|---|---|---|---|
| | | Sum of squares | *F* ratio | *p*-value | Sum of squares | *F* ratio | *p*-value |
| Micronuclei | | | | | | | |
| Dose | 1 | 14,081.0 | 79.2 | < 0.0001 | 1,590.5 | 51.7 | < 0.0001 |
| Cell line | 1 | 1,321.0 | 7.4 | 0.012 | 1,136.7 | 36.9 | < 0.0001 |
| $O_2$ level | 5 | 33,542.8 | 37.7 | < 0.0001 | 2,003.3 | 13.0 | < 0.0001 |
| Dose * Cell line | 1 | 0.05 | 0.0003 | 0.99 | 17.2 | 0.6 | 0.46 |
| Dose * $O_2$ level | 5 | 7,208.0 | 8.1 | < 0.0001 | 251.7 | 1.6 | 0.19 |
| Cell line * $O_2$ level | 5 | 1,883.2 | 2.1 | 0.10 | 1,555.6 | 10.1 | < 0.0001 |
| Dose * Cell line * $O_2$ level | 5 | 275.6 | 0.3 | 0.90 | 238.9 | 1.6 | 0.21 |
| Bridges | | | | | | | |
| Dose | 1 | 1,340.5 | 28.8 | < 0.0001 | 72.1 | 10.3 | 0.004 |
| Cell line | 1 | 879.3 | 18.9 | 0.0002 | 173.5 | 24.7 | < 0.0001 |
| $O_2$ level | 5 | 7,261.9 | 31.2 | < 0.0001 | 219.2 | 6.2 | 0.0008 |
| Dose * Cell line | 1 | 7.6 | 0.2 | 0.69 | 0.5 | 0.1 | 0.79 |
| Dose * $O_2$ level | 5 | 1,446.1 | 6.2 | 0.0008 | 90.1 | 2.6 | 0.054 |
| Cell line * $O_2$ level | 5 | 391.0 | 1.7 | 0.18 | 90.6 | 2.6 | 0.053 |
| Dose * Cell line * $O_2$ level | 5 | 141.1 | 0.6 | 0.70 | 22.4 | 0.6 | 0.67 |

**Table 3.5. Multivariate analyses of 40 - 100 cGy dose response in G2 and G1**

| Source | df | G2 | | | G1 | | |
|---|---|---|---|---|---|---|---|
| | | Sum of squares | *F* ratio | *p*-value | Sum of squares | *F* ratio | *p*-value |
| Micronuclei | | | | | | | |
| Dose | 1 | 12,251.5 | 324.3 | < 0.0001 | 11,774.8 | 155.8 | < 0.0001 |
| Cell line | 1 | 685.7 | 18.1 | 0.0003 | 4.6 | 0.1 | 0.0808 |
| $O_2$ level | 5 | 32,678.2 | 173.0 | < 0.0001 | 12,050.9 | 31.9 | < 0.0001 |
| Dose * Cell line | 1 | 3.2 | 0.1 | 0.77 | 113.8 | 1.5 | 0.23 |
| Dose * $O_2$ level | 5 | 1,859.0 | 9.8 | < 0.0001 | 1,133.1 | 3.0 | 0.03 |
| Cell line * $O_2$ level | 5 | 2,874.6 | 15.2 | < 0.0001 | 2,335.5 | 6.2 | 0.0008 |
| Dose * Cell line * $O_2$ level | 5 | 673.8 | 3.6 | 0.015 | 521.1 | 1.4 | 0.27 |
| Bridges | | | | | | | |
| Dose | 1 | 231.8 | 11.6 | 0.0023 | 410.1 | 26.2 | < 0.0001 |
| Cell line | 1 | 502.2 | 25.1 | < 0.0001 | 177.4 | 11.4 | 0.003 |
| $O_2$ level | 5 | 6,298.3 | 63.0 | < 0.0001 | 1,232.6 | 15.8 | < 0.0001 |
| Dose * Cell line | 1 | 68.6 | 3.4 | 0.08 | 0.01 | 0.0004 | 0.98 |
| Dose * $O_2$ level | 5 | 69.2 | 0.7 | 0.63 | 277.2 | 3.5 | 0.02 |
| Cell line * $O_2$ level | 5 | 488.8 | 4.9 | 0.0032 | 334.5 | 4.3 | 0.01 |
| Dose * Cell line * $O_2$ level | 5 | 379.0 | 3.79 | 0.011 | 163.8 | 2.1 | 0.10 |

**Table 3.6. Multivariate analyses of 200 - 400 cGy dose responses in G2 and G1**

| Source | df | G2 | | | G1 | | |
|---|---|---|---|---|---|---|---|
| | | Sum of squares | *F* ratio | *p*-value | Sum of squares | *F* ratio | *p*-value |
| Micronuclei | | | | | | | |
| Dose | 1 | 151.9 | 0.3 | 0.60 | 298.1 | 0.7 | 0.42 |
| Cell line | 1 | 211.5 | 0.4 | 0.54 | 1,014.0 | 2.5 | 0.16 |
| $O_2$ level | 5 | 13,383.6 | 13.5 | 0.006 | 29,466.6 | 36.5 | 0.0004 |
| Dose * Cell line | 1 | 1,380.0 | 2.8 | 0.15 | 215.8 | 0.5 | 0.49 |
| Dose * $O_2$ level | 5 | 1,520.5 | 1.5 | 0.29 | 1,027.8 | 1.3 | 0.35 |
| Cell line * $O_2$ level | 5 | 5,012.8 | 5.1 | 0.05 | 263.2 | 0.3 | 0.73 |
| Dose * Cell line * $O_2$ level | 5 | 3,013.4 | 3.0 | 0.12 | 65.2 | 0.1 | 0.92 |
| Bridges | | | | | | | |
| Dose | 1 | 58.0 | 3.1 | 0.13 | 260.4 | 1.7 | 0.24 |
| Cell line | 1 | 17.6 | 1.0 | 0.37 | 285.8 | 1.8 | 0.23 |
| $O_2$ level | 5 | 3,324.1 | 89.6 | 0.0001 | 626.0 | 2.0 | 0.22 |
| Dose * Cell line | 1 | 263.0 | 14.2 | 0.009 | 17.4 | 0.1 | 0.75 |
| Dose * $O_2$ level | 5 | 91.9 | 2.5 | 0.16 | 83.2 | 0.3 | 0.78 |
| Cell line * $O_2$ level | 5 | 90.2 | 2.4 | 0.17 | 1,082.7 | 3.5 | 0.10 |
| Dose * Cell line * $O_2$ level | 5 | 17.6 | 0.47 | 0.64 | 722.3 | 2.3 | 0.18 |

Due to the high levels of statistical significance seen for $O_2$ in the multivariate analyses, post-hoc tests were performed on the $O_2$ treatment levels (Table 3.7). These analyses indicate which $O_2$ levels differed from others in each of the three dose ranges, 0 - 20 cGy, 40 – 100 cGy and 200 – 400 cGy. For MN, cells irradiated at all three dose ranges in G2 showed that responses in ambient air, the centrifuge control, and post-irradiation re-oxygenation were all different from the responses at 2.5%, 5%, and post-irradiation hypo-oxygenation. However, in G1 the $O_2$ treatment groups partially overlapped in their responses at dose ranges 0 – 20 cGy and 40 – 100 cGy, but not at 200 – 400 cGy. For bridges, the responses of cells irradiated in G2 in ambient air, the centrifuge control, and post-irradiation re-oxygenation were distinguishable from one another, but overall these responses clearly differed from those at 2.5%, 5%, and post-irradiation hypo-oxygenation in all three dose ranges. In G1 the responses for bridges at all $O_2$ levels showed more overlapping for the lower two dose ranges than was seen for MN, but at 200 – 400 cGy the $O_2$ responses were statistically indistinguishable.

Overall, these results clearly show lower frequencies of MN and bridges at low $O_2$ levels in G1- and G2-irradiated cells in all three dose ranges compared to ambient air. G2-irradiated cells exhibited a loss of HRS at 0 - 20 cGy at low $O_2$ compared to ambient air. Post-irradiation re-oxygenation of the G2-irradiated cells, led to reinstatement of the HRS effects at 0 - 20 cGy and an increase in cytogenetic damage for dose groups 40 – 100 and 200 – 300 cGy. In contrast, the post-irradiation hypo-oxygenation results indicate loss of the G2-specific HRS effect at 0 - 20 cGy and an

**Table 3.7. Post Hoc test results of the $O_2$ treatment conditions for all dose groups for MN and Bridges in cells irradiated in G2 or G1.**

| Source | Micronuclei | | | | Bridges | | | |
|---|---|---|---|---|---|---|---|---|
| | G2 | | G1 | | G2 | | G1 | |
| O2 treatment condition | Treatment group levels[a] | Least Squares Mean | Treatment group levels[a] | Least Squares Mean | Treatment group levels[a] | Least Squares Mean | Treatment group levels[a] | Least Squares Mean |
| 0 - 20 cGy | | | | | | | | |
| Ambient air | A | 103.1 | A | 42.0 | A | 38.4 | A | 10.5 |
| Centrifuge | A | 92.3 | B C | 32.7 | A | 39.9 | A | 8.9 |
| Re-oxygenation | A | 84.3 | A B | 34.1 | B | 23.6 | A | 7.9 |
| 2.5% | B | 52.2 | D | 22.1 | B C | 19.7 | A B | 7.1 |
| 5% | B | 40.5 | B C D | 28.6 | C D | 11.1 | A B | 6.8 |
| Hypo-oxygenation | B | 34.9 | C D | 25.4 | D | 7.7 | B | 3.5 |
| 40 - 100 cGy | | | | | | | | |
| Ambient air | A | 135.9 | A | 83.9 | A | 40.1 | A | 22.4 |
| Centrifuge | B | 121.7 | A B | 72.8 | A | 39.3 | A B | 19.1 |
| Re-oxygenation | B | 114.3 | A | 82.8 | B | 27.9 | B | 16.7 |
| 2.5% | C | 70.7 | C | 53.7 | C | 19.6 | B | 14.0 |
| 5% | C | 77.1 | B C | 60.1 | C D | 14.8 | A B | 13.8 |
| Hypo-oxygenation | C | 72.7 | D | 39.8 | D | 10.4 | C | 6.1 |
| 200 - 400 cGy[b] | | | | | | | | |
| Ambient air | A | 184.4 | A | 202.1 | A | 54.4 | A | 44.7 |
| 2.5% | B | 135.3 | B | 109.5 | B | 31.5 | A | 34.0 |
| 5% | B | 120.6 | B | 125.2 | C | 22.0 | A | 31.0 |

a: Treatment group levels not connected by the same letter are significantly different from each other.
b: Not all $O_2$ levels were evaluated at high doses.

overall reduction in cytogenetic damage for all three dose ranges. The G1-irradiated cells did not exhibit HRS at 0 – 20 cGy. Taken together these results indicate that cytogenetic damage is lower when cells are recovering from radiation exposure under conditions of low $O_2$ than when cells are cultured in ambient $O_2$.

## DISCUSSION

Recently we observed HRS at doses ≤ 20 cGy in four normal human lymphoblastoid cell lines that had been irradiated with Cobalt-60 gamma rays (Joshi et al. 2014). HRS is a well-known G2-specific low-dose radiation response, however the mechanism of HRS is not very well understood, and prior to our previous work HRS had not been observed with a cytogenetic endpoint. In the present study we cultured and irradiated cells in either ambient air (21%) $O_2$, 2.5% $O_2$, or 5% $O_2$. For cells irradiated in G2, a lack of HRS is evident at ≤ 20 cGy at low $O_2$ levels compared to cells cultured and irradiated in ambient air (Figures 1 and 2). These results are highly statistically significant for MN and for bridges (Table 3.4; $p < 0.0001$). However, G1-irradiated cells did not show the low dose specific HRS response at any $O_2$ level for either cell line. A previous study used a clonogenic cell survival assay and showed the loss of HRS at 4% $O_2$ with T-47D (human breast carcinoma) cells (Edin et al. 2012). Here we studied the effects of equilibrating cells at 2.5% and 5% $O_2$ before and immediately after irradiation, and then evaluated the cells for cytogenetic damage 2 hours (G2 phase) or 22 hours (G1 phase) later. This study provides the first cytogenetic evidence for the loss of HRS at low $O_2$ levels in G2-irradiated normal human lymphoblastoid cells.

We further evaluated whether the lack of an HRS response in G2 cells was due to low $O_2$ either prior or after irradiation. Since we observed a loss of HRS at 5% $O_2$, which is the approximate physiological $O_2$ concentration, we studied the effects of re-oxygenation to ambient air immediately following exposure in cells that were irradiated at 5% $O_2$. The results indicate that the HRS response is reinstated in G2-irradiated cells when re-oxygenation to ambient air begins immediately after exposure and continues

until the time of harvest. This return of HRS is similar to the response following G2-irradiation for both cell lines when they were cultured, irradiated and maintained in ambient air throughout the entire experiment. These results indicate that reinstatement of HRS (Figures 3 and 4) is due to the return to ambient $O_2$ concentration following irradiation at 5% $O_2$ levels. Previous studies have demonstrated that re-oxygenation leads to increased intracellular reactive oxygen species (ROS) causing direct damage to DNA (Brown 1999; Overgaard 2007). Re-oxygenation of tumor cells is also known to alter the effectiveness of DNA repair processes through activation of a hypoxia inducible factor (Bristow and Hill 2008; Olcina et al. 2010; Pires et al. 2012). Based on these previous studies, the HRS response observed in our G2-irradiated cells upon post-irradiation re-oxygenation may be due, at least in part, to elevated levels of ROS.

To evaluate further the role of $O_2$ after irradiation, we hypo-oxygenated cells to 5% $O_2$ that had been cultured and subsequently irradiated in ambient air. Hypo-oxygenation resulted in a significantly diminished HRS effect in G2-irradiated cells for both cell lines (Figures 3 and 4). These findings suggest that reduced $O_2$ levels post-irradiation result either in reduced DNA damage due to diminished ROS, or that the ATM-mediated DNA damage repair pathway is activated. Activation of the ATM pathway is mediated through a complex containing MRE11, RAD50, and NBS1 (MRN complex) (Bencokova et al. 2009; Thompson 2012)

Multivariate regression analyses of the data presented here indicate that for MN and bridges, low $O_2$ levels post-irradiation lead to the loss of HRS in G2 cells irradiated at 0 - 20 cGy (Table 3.4). Regression analyses also revealed an overall reduction in the frequencies of both MN and bridges in G1-irradiated cells (Table 3.4) at doses 0 -20

cGy. Overall, for both MN and bridges, $O_2$ effects were also observed at dose groups 40 – 100 cGy and 200 – 300 cGy in both G2 and G1 irradiated cells (Tables 3.5 and 3.6). The post-hoc tests indicate that for MN at all three dose ranges, the $O_2$ treatment groups for G2-irradiated cells in ambient air, centrifuge control and post-irradiation re-oxygenation are significantly different than when these cells are irradiated in 2.5%, 5% and post-irradiation hypo-oxygenation (Table 3.7). However, for MN the responses of the G1-irradiated cells overlap at all $O_2$ levels and for all dose ranges. Taken together, the multivariate analyses and the post-hoc tests confirm that for MN the cytogenetic response of G2-irradiated cells is reduced in atmospheres of 2.5% and 5% $O_2$, and in post-irradiation hypo-oxygenation compared to the responses of the same cells in ambient air, centrifuge control and post-irradiation re-oxygenation. For bridges at all three dose ranges, the responses of G2- and G1-irradiated cells in ambient air, centrifuge control and post-irradiation re-oxygenation are significantly different than when the cells are irradiated in atmospheres of 2.5% $O_2$, 5% $O_2$, and in post-irradiation hypo-oxygenation, however these responses overlap within each group (Table 3.7).

The results indicate that in both G2 and G1 phases of the cell cycle, a reduction in the frequencies of MN and bridges is observed when normal human lymphoblastoid cells are cultured and irradiated at 0 – 400 cGy in 2.5% or 5% $O_2$. The G2-specific low dose HRS response in ambient air is lost when cells are irradiated at 0 - 20 cGy in 2.5% and 5% $O_2$ while the HRS response is reinstated upon re-oxygenation to ambient $O_2$ levels. Cells irradiated in G1 did not exhibit HRS for any dose range at any $O_2$ level tested here. Since many solid tumors are differentially oxygenated, our results suggest that tumor hypo-oxygenation may be of interest for enhancing the radiation therapy.

## REFERENCES

1. Albertini RJ, Anderson D, Douglas GR, Hagmar L, Hemminki K, Merlo F, Natarajan AT, Norppa H, Shuker DE, Tice R, Waters MD, Aitio A. 2000. IPCS guidelines for the monitoring of genotoxic effects of carcinogens in humans. International Programme on Chemical Safety. Mutation Research 463(2):111-172.

2. Aypar U, Morgan WF, Baulch JE. 2011. Radiation-induced genomic instability: are epigenetic mechanisms the missing link? International Journal of Radiation Biology 87(2):179-191.

3. Bakkenist CJ, Kastan MB. 2003. DNA damage activates ATM through intermolecular autophosphorylation and dimer dissociation. Nature 421(6922):499-506.

4. Bencokova Z, Kaufmann MR, Pires IM, Lecane PS, Giaccia AJ, Hammond EM. 2009. ATM activation and signaling under hypoxic conditions. Molecular and Cellular Biology 29(2):526-537.

5. Bhatti P, Yong LC, Doody MM, Preston DL, Kampa DM, Ramsey MJ, Ward EM, Edwards AA, Ron E, Tucker JD, Sigurdson AJ. 2010. Diagnostic X-ray examinations and increased chromosome translocations: evidence from three studies. Radiation and Environmental Biophysics 49(4):685-692.

6. Bond VP, Cronkite EP. 1957. Effects of radiation on mammals. Annual Review of Physiology 19:299-328.

7. Boregowda SV, Krishnappa V, Chambers JW, Lograsso PV, Lai WT, Ortiz LA, Phinney DG. 2012. Atmospheric oxygen inhibits growth and differentiation of

marrow-derived mouse mesenchymal stem cells via a p53-dependent mechanism: implications for long-term culture expansion. Stem Cells 30(5):975-987.

8. Brenner DJ, Doll R, Goodhead DT, Hall EJ, Land CE, Little JB, Lubin JH, Preston DL, Preston RJ, Puskin JS, Ron E, Sachs RK, Samet JM, Setlow RB, Zaider M. 2003. Cancer risks attributable to low doses of ionizing radiation: assessing what we really know. Proceedings of the National Academy of Sciences of the United States of America 100(24):13761-13766.

9. Brenner DJ, Hall EJ. 2007. Computed tomography--an increasing source of radiation exposure. The New England Journal of Medicine 357(22):2277-2284.

10. Bristow RG, Hill RP. 2008. Hypoxia and metabolism. Hypoxia, DNA repair and genetic instability. Nature Reviews Cancer 8(3):180-192.

11. Brown JM. 1999. The hypoxic cell: a target for selective cancer therapy--eighteenth Bruce F. Cain Memorial Award lecture. Cancer Research 59(23):5863-5870.

12. Brown JM. 2002. Tumor microenvironment and the response to anticancer therapy. Cancer Biology & Therapy 1(5):453-458.

13. Brown JM, Diehn M, Loo BW, Jr. 2010. Stereotactic ablative radiotherapy should be combined with a hypoxic cell radiosensitizer. International Journal of Radiation Oncology, Biology, Physics 78(2):323-327.

14. Buscemi G, Perego P, Carenini N, Nakanishi M, Chessa L, Chen J, Khanna K, Delia D. 2004. Activation of ATM and Chk2 kinases in relation to the amount of DNA strand breaks. Oncogene 23(46):7691-7700.

15. Cam H, Easton JB, High A, Houghton PJ. 2010. mTORC1 signaling under hypoxic conditions is controlled by ATM-dependent phosphorylation of HIF-1alpha. Molecular Cell 40(4):509-520.

16. Canman CE, Lim DS. 1998. The role of ATM in DNA damage responses and cancer. Oncogene 17(25):3301-3308.

17. Cardis E, Gilbert ES, Carpenter L, Howe G, Kato I, Armstrong BK, Beral V, Cowper G, Douglas A, Fix J, et al. 1995. Effects of low doses and low dose rates of external ionizing radiation: cancer mortality among nuclear industry workers in three countries. Radiation Research 142(2):117-132.

18. Cardis E, Vrijheid M, Blettner M, Gilbert E, Hakama M, Hill C, Howe G, Kaldor J, Muirhead CR, Schubauer-Berigan M, Yoshimura T, Bermann F, Cowper G, Fix J, Hacker C, Heinmiller B, Marshall M, Thierry-Chef I, Utterback D, Ahn YO, Amoros E, Ashmore P, Auvinen A, Bae JM, Bernar J, Biau A, Combalot E, Deboodt P, Diez Sacristan A, Eklof M, Engels H, Engholm G, Gulis G, Habib RR, Holan K, Hyvonen H, Kerekes A, Kurtinaitis J, Malker H, Martuzzi M, Mastauskas A, Monnet A, Moser M, Pearce MS, Richardson DB, Rodriguez-Artalejo F, Rogel A, Tardy H, Telle-Lamberton M, Turai I, Usel M, Veress K. 2007. The 15-Country Collaborative Study of Cancer Risk among Radiation Workers in the Nuclear Industry: estimates of radiation-related cancer risks. Radiation Research 167(4):396-416.

19. Cheong HS, Seth I, Joiner MC, Tucker JD. 2013. Relationships among micronuclei, nucleoplasmic bridges and nuclear buds within individual cells in the cytokinesis-block micronucleus assay. Mutagenesis 28(4):433-440.

20. Cronkite EP, Bond VP, Chapman WH, Lee RH. 1955. Biological effect of atomic bomb gamma radiation. Science 122(3160):148-150.

21. Curtis RE FD RE, Ries LAG, Hacker DG, Edwards BK, Tucker MA, Fraumeni JF Jr. . 2006. Malignancies Among Cancer Survivors: SEER Cancer Registries, 1973-2000. National Cancer Institute.

22. Day TK, Zeng G, Hooker AM, Bhat M, Turner DR, Sykes PJ. 2007. Extremely low doses of X-radiation can induce adaptive responses in mouse prostate. Dose-Response : A Publication of International Hormesis Society 5(4):315-322.

23. Dilworth JT, Krueger SA, Dabjan M, Grills IS, Torma J, Wilson GD, Marples B. 2013. Pulsed low-dose irradiation of orthotopic glioblastoma multiforme (GBM) in a pre-clinical model: effects on vascularization and tumor control. Radiotherapy and Oncology : Journal of the European Society for Therapeutic Radiology and Oncology 108(1):149-154.

24. Douple EB, Mabuchi K, Cullings HM, Preston DL, Kodama K, Shimizu Y, Fujiwara S, Shore RE. 2011. Long-term radiation-related health effects in a unique human population: lessons learned from the atomic bomb survivors of Hiroshima and Nagasaki. Disaster Medicine and Public Health Preparedness 5 Suppl 1:S122-133.

25. Eastmond DA, Tucker JD. 1989a. Identification of aneuploidy-inducing agents using cytokinesis-blocked human lymphocytes and an antikinetochore antibody. Environmental and Molecular Mutagenesis 13(1):34-43.

26. Eastmond DA, Tucker JD. 1989b. Kinetochore localization in micronucleated cytokinesis-blocked Chinese hamster ovary cells: a new and rapid assay for identifying aneuploidy-inducing agents. Mutation Research 224(4):517-525.

27. Edin NJ, Olsen DR, Sandvik JA, Malinen E, Pettersen EO. 2012. Low dose hyper-radiosensitivity is eliminated during exposure to cycling hypoxia but returns after reoxygenation. International Journal of Radiation Biology 88(4):311-319.

28. Enns L, Bogen KT, Wizniak J, Murtha AD, Weinfeld M. 2004. Low-dose radiation hypersensitivity is associated with p53-dependent apoptosis. Molecular Cancer Research: MCR 2(10):557-566.

29. Fenech M. 2000. The in vitro micronucleus technique. Mutation Research 455(1-2):81-95.

30. Fenech M, Bonassi S, Turner J, Lando C, Ceppi M, Chang WP, Holland N, Kirsch-Volders M, Zeiger E, Bigatti MP, Bolognesi C, Cao J, De Luca G, Di Giorgio M, Ferguson LR, Fucic A, Lima OG, Hadjidekova VV, Hrelia P, Jaworska A, Joksic G, Krishnaja AP, Lee TK, Martelli A, McKay MJ, Migliore L, Mirkova E, Muller WU, Odagiri Y, Orsiere T, Scarfi MR, Silva MJ, Sofuni T, Surralles J, Trenta G, Vorobtsova I, Vral A, Zijno A. 2003. Intra- and inter-laboratory variation in the scoring of micronuclei and nucleoplasmic bridges in binucleated human lymphocytes. Results of an international slide-scoring exercise by the HUMN project. Mutation Research 534(1-2):45-64.

31. Fenech M, Kirsch-Volders M, Natarajan AT, Surralles J, Crott JW, Parry J, Norppa H, Eastmond DA, Tucker JD, Thomas P. 2011. Molecular mechanisms of

micronucleus, nucleoplasmic bridge and nuclear bud formation in mammalian and human cells. Mutagenesis 26(1):125-132.

32. Fuglede NB, Brinck-Claussen UO, Deltour I, Boesen EH, Dalton SO, Johansen C. 2011. Incidence of cutaneous malignant melanoma in Denmark, 1978-2007. The British Journal of Dermatology.

33. Garcia-Barros M, Paris F, Cordon-Cardo C, Lyden D, Rafii S, Haimovitz-Friedman A, Fuks Z, Kolesnick R. 2003. Tumor response to radiotherapy regulated by endothelial cell apoptosis. Science 300(5622):1155-1159.

34. Gudkov AV, Komarova EA. 2007. Dangerous habits of a security guard: the two faces of p53 as a drug target. Human Molecular Genetics 16 Spec No 1:R67-72.

35. Hamada N, Schettino G, Kashino G, Vaid M, Suzuki K, Kodama S, Vojnovic B, Folkard M, Watanabe M, Michael BD, Prise KM. 2006. Histone H2AX phosphorylation in normal human cells irradiated with focused ultrasoft X rays: evidence for chromatin movement during repair. Radiation Research 166(1 Pt 1):31-38.

36. Han J, Won EJ, Lee BY, Hwang UK, Kim IC, Yim JH, Leung KM, Lee YS, Lee JS. 2014. Gamma rays induce DNA damage and oxidative stress associated with impaired growth and reproduction in the copepod Tigriopus japonicus. Aquatic Toxicology 152:264-272.

37. Hanahan D, Weinberg RA. 2011. Hallmarks of Cancer: The Next Generation. Cell 144(5):646-674.

38. Helleday T, Petermann E, Lundin C, Hodgson B, Sharma RA. 2008. DNA repair pathways as targets for cancer therapy. Nature Reviews Cancer 8(3):193-204.

39. Henderson BW, Miller AC. 1986. Effects of scavengers of reactive oxygen and radical species on cell survival following photodynamic treatment in vitro: comparison to ionizing radiation. Radiation Research 108(2):196-205.

40. Hill MA. 2004. The variation in biological effectiveness of X-rays and gamma rays with energy. Radiation Protection Dosimetry 112(4):471-481.

41. Hockel M, Vaupel P. 2001. Tumor hypoxia: definitions and current clinical, biologic, and molecular aspects. Journal of the National Cancer Institute 93(4):266-276.

42. Hockel M, Vorndran B, Schlenger K, Baussmann E, Knapstein PG. 1993. Tumor oxygenation: a new predictive parameter in locally advanced cancer of the uterine cervix. Gynecologic Oncology 51(2):141-149.

43. ICRP. 1991. Recommendations of the International Commission on Radiological Protection. Internation Council of Radiation Protection.

44. Jeggo PA. 2009. Risks from low dose/dose rate radiation: what an understanding of DNA damage response mechanisms can tell us. Health Physics 97(5):416-425.

45. Joiner M, Marples B, Lambin P, Short S, Turesson I. 2001a. Low-dose hypersensitivity: Current status and possible mechanisms. International Journal of Radiation Oncology, Biology, Physics 49:379-389.

46. Joiner MC, Johns H. 1988. Renal damage in the mouse: the response to very small doses per fraction. Radiation Research 114(2):385-398.

47. Joiner MC, Lambin P, Malaise EP, Robson T, Arrand JE, Skov KA, Marples B. 1996. Hypersensitivity to very-low single radiation doses: Its relationship to the

adaptive response and induced radioresistance. Mutation Research 358:171-183.

48. Joiner MC, Marples B, Johns H. 1993. The response of tissues to very low doses per fraction: a reflection of induced repair? Recent Results in Cancer Research Fortschritte der Krebsforschung Progres dans les recherches sur le cancer 130:27-40.

49. Joiner MC, Marples B, Lambin P, Short SC, Turesson I. 2001b. Low-dose hypersensitivity: current status and possible mechanisms. International Journal of Radiation Oncology, Biology, Physics 49(2):379-389.

50. Jones IM, Galick H, Kato P, Langlois RG, Mendelsohn ML, Murphy GA, Pleshanov P, Ramsey MJ, Thomas CB, Tucker JD, Tureva L, Vorobtsova I, Nelson DO. 2002. Three somatic genetic biomarkers and covariates in radiation-exposed Russian cleanup workers of the chernobyl nuclear reactor 6-13 years after exposure. Radiation Research 158(4):424-442.

51. Joshi GS, Joiner MC, Tucker JD. 2014. Cytogenetic characterization of low-dose hyper-radiosensitivity in Cobalt-60 irradiated human lymphoblastoid cells. Submitted.

52. Kinner A, Wu W, Staudt C, Iliakis G. 2008. Gamma-H2AX in recognition and signaling of DNA double-strand breaks in the context of chromatin. Nucleic Acids Research 36(17):5678-5694.

53. Kleinerman RA, Tucker MA, Tarone RE, Abramson DH, Seddon JM, Stovall M, Li FP, Fraumeni JF, Jr. 2005. Risk of new cancers after radiotherapy in long-term

survivors of retinoblastoma: an extended follow-up. Journal of Clinical Oncology : Official Journal of the American Society of Clinical Oncology 23(10):2272-2279.

54. Koukourakis MI. 2012. Radiation damage and radioprotectants: new concepts in the era of molecular medicine. The British Journal of Radiology 85(1012):313-330.

55. Krempler A, Deckbar D, Jeggo PA, Lobrich M. 2007. An imperfect G2M checkpoint contributes to chromosome instability following irradiation of S and G2 phase cells. Cell Cycle 6(14):1682-1686.

56. Krueger SA, Collis SJ, Joiner MC, Wilson GD, Marples B. 2007a. Transition in survival from low-dose hyper-radiosensitivity to increased radioresistance is independent of activation of ATM SER1981 activity. International Journal of Radiation Oncology, Biology, Physics 69(4):1262-1271.

57. Krueger SA, Joiner MC, Weinfeld M, Piasentin E, Marples B. 2007b. Role of apoptosis in low-dose hyper-radiosensitivity. Radiation Research 167(3):260-267.

58. Krueger SA, Wilson GD, Piasentin E, Joiner MC, Marples B. 2010. The effects of G2-phase enrichment and checkpoint abrogation on low-dose hyper-radiosensitivity. International Journal of Radiation Oncology, Biology, Physics 77(5):1509-1517.

59. Lambin P, Coco-Martin J, Legal JD, Begg AC, Parmentier C, Joiner MC, Malaise EP. 1994. Intrinsic radiosensitivity and chromosome aberration analysis using fluorescence in situ hybridization in cells of two human tumor cell lines. Radiation research 138(1 Suppl):S40-43.

60. Leung SW, Lee TF, Chien CY, Chao PJ, Tsai WL, Fang FM. 2011. Health-related Quality of life in 640 head and neck cancer survivors after radiotherapy using EORTC QLQ-C30 and QLQ-H&N35 questionnaires. BMC Cancer 11(1):128.

61. Lilienfeld A, Pedersen E, Dowd J. 1967. Cancer Epidemiology: Methods of Study. Baltimore: The Johns Hopkins University Press.

62. Little JB. 2006. Lauriston S. Taylor lecture: nontargeted effects of radiation: implications for low-dose exposures. Health Physics 91(5):416-426.

63. Little MP. 2009. Cancer and non-cancer effects in Japanese atomic bomb survivors. Journal of Radiological Protection : Official Journal of the Society for Radiological Protection 29(2A):A43-59.

64. Lobrich M, Jeggo PA. 2005. The two edges of the ATM sword: co-operation between repair and checkpoint functions. Radiotherapy and Oncology : Journal of the European Society for Therapeutic Radiology and Oncology 76(2):112-118.

65. Ma NY, Tinganelli W, Maier A, Durante M, Kraft-Weyrather W. 2013. Influence of chronic hypoxia and radiation quality on cell survival. Journal of Radiation Research 54 Suppl 1:i13-22.

66. Mahaney BL, Meek K, Lees-Miller SP. 2009. Repair of ionizing radiation-induced DNA double-strand breaks by non-homologous end-joining. The Biochemical Journal 417(3):639-650.

67. Marples B. 2004. Is low-dose hyper-radiosensitivity a measure of G2-phase cell radiosensitivity? Cancer Metastasis Reviews 23(3-4):197-207.

68. Marples B, Collis SJ. 2008. Low-dose hyper-radiosensitivity: past, present, and future. International Journal of Radiation Oncology, Biology, Physics 70(5):1310-1318.

69. Marples B, Joiner MC. 1993. The response of Chinese hamster V79 cells to low radiation doses: evidence of enhanced sensitivity of the whole cell population. Radiation Research 133(1):41-51.

70. Marples B, Joiner MC, Skov KA. 1994a. The effect of oxygen on low-dose hypersensitivity and increased radioresistance in Chinese hamster V79-379A cells. Radiation Research 138(1 Suppl):S17-20.

71. Marples B, Lam GK, Zhou H, Skov KA. 1994b. The response of Chinese hamster V79-379A cells exposed to negative pi-mesons: evidence that increased radioresistance is dependent on linear energy transfer. Radiation Research 138(1 Suppl):S81-84.

72. Marples B, Wouters BG, Collis SJ, Chalmers AJ, Joiner MC. 2004. Low-dose hyper-radiosensitivity: a consequence of ineffective cell cycle arrest of radiation-damaged G2-phase cells. Radiation Research 161(3):247-255.

73. Marples B, Wouters BG, Joiner MC. 2003. An association between the radiation-induced arrest of G2-phase cells and low-dose hyper-radiosensitivity: a plausible underlying mechanism? Radiation Research 160(1):38-45.

74. Martin LM, Marples B, Lynch TH, Hollywood D, Marignol L. 2013. Exposure to low dose ionising radiation: molecular and clinical consequences. Cancer Letters 338(2):209-218.

75. Mettler FA, Jr., Gus'kova AK, Gusev I. 2007. Health effects in those with acute radiation sickness from the Chernobyl accident. Health Physics 93(5):462-469.

76. Mitchel RE. 2007. Cancer and low dose responses in vivo: implications for radiation protection. Dose-response : A Publication of International Hormesis Society 5(4):284-291.

77. Mongiardi MP, Stagni V, Natoli M, Giaccari D, D'Agnano I, Falchetti ML, Barila D, Levi A. 2011. Oxygen sensing is impaired in ATM-defective cells. Cell Cycle 10(24):4311-4320.

78. Moore DH, 2nd, Tucker JD, Jones IM, Langlois RG, Pleshanov P, Vorobtsova I, Jensen R. 1997. A study of the effects of exposure on cleanup workers at the Chernobyl nuclear reactor accident using multiple end points. Radiation Research 148(5):463-475.

79. Moore ID, Tucker JD. 1999. Biological dosimetry of chernobyl cleanup workers: inclusion of data on age and smoking provides improved radiation dose estimates. Radiation Research 152(6):655-664.

80. Morgan WF, Bair WJ. 2013. Issues in low dose radiation biology: the controversy continues. A perspective. Radiation Research 179(5):501-510.

81. Moulder JE, Rockwell S. 1987. Tumor hypoxia: its impact on cancer therapy. Cancer Metastasis Reviews 5(4):313-341.

82. NCRP. 2009. Ionizing radiation exposure of the population of the United States: 2006. NCRP Report No. 160. Bathesda, MD: National Council on Radiation Protection and Measurements., 2009. National Council on Radiation Protection.

83. Noda A, Hirai Y, Hamasaki K, Mitani H, Nakamura N, Kodama Y. 2012. Unrepairable DNA double-strand breaks that are generated by ionising radiation determine the fate of normal human cells. Journal of Cell Science 125(Pt 22):5280-5287.

84. Olcina M, Lecane PS, Hammond EM. 2010. Targeting hypoxic cells through the DNA damage response. Clinical Cancer Research : An Official Journal of the American Association for Cancer Research 16(23):5624-5629.

85. Ostroumova E, Gudzenko N, Brenner A, Gorokh Y, Hatch M, Prysyazhnyuk A, Mabuchi K, Bazyka D. 2014. Thyroid cancer incidence in Chornobyl liquidators in Ukraine: SIR analysis, 1986-2010. European Journal of Epidemiology 29(5):337-342.

86. Overgaard J. 2007. Hypoxic radiosensitization: adored and ignored. Journal of Clinical Oncology : Official Journal of the American Society of Clinical Oncology 25(26):4066-4074.

87. Palcic B, Brosing JW, Skarsgard LD. 1982. Survival measurements at low doses: oxygen enhancement ratio. British Journal of Cancer 46(6):980-984.

88. Parker C, Milosevic M, Toi A, Sweet J, Panzarella T, Bristow R, Catton C, Catton P, Crook J, Gospodarowicz M, McLean M, Warde P, Hill RP. 2004. Polarographic electrode study of tumor oxygenation in clinically localized prostate cancer. International Journal of Radiation Oncology, Biology, Physics 58(3):750-757.

89. Pettersen EO, Bjorhovde I, Sovik A, Edin NF, Zachar V, Hole EO, Sandvik JA, Ebbesen P. 2007. Response of chronic hypoxic cells to low dose-rate irradiation. International Journal of Radiation Biology 83(5):331-345.

90. Pierce DA, Preston DL. 2000. Radiation-related cancer risks at low doses among atomic bomb survivors. Radiation Research 154(2):178-186.

91. Pierquin B, Tubiana M, Pan C, Lagrange JL, Calitchi E, Otmezguine Y. 2007. Long-term results of breast cancer irradiation treatment with low-dose-rate external irradiation. International journal of Radiation Oncology, Biology, Physics 67(1):117-121.

92. Pires IM, Olcina MM, Anbalagan S, Pollard JR, Reaper PM, Charlton PA, McKenna WG, Hammond EM. 2012. Targeting radiation-resistant hypoxic tumour cells through ATR inhibition. British Journal of Cancer 107(2):291-299.

93. Prise KM. 2006. New advances in radiation biology. Occupational Medicine 56(3):156-161.

94. Reeves GI. 1999. Radiation injuries. Critical Care Clinics 15(2):457-473.

95. Robertson CA, Evans DH, Abrahamse H. 2009. Photodynamic therapy (PDT): a short review on cellular mechanisms and cancer research applications for PDT. Journal of Photochemistry and Photobiology B, Biology 96(1):1-8.

96. Rockwell S, Dobrucki IT, Kim EY, Marrison ST, Vu VT. 2009. Hypoxia and radiation therapy: past history, ongoing research, and future promise. Current Molecular Medicine 9(4):442-458.

97. Rothkamm K, Lobrich M. 2003. Evidence for a lack of DNA double-strand break repair in human cells exposed to very low x-ray doses. Proceedings of the

National Academy of Sciences of the United States of America 100(9):5057-5062.

98. Ryan LA, Smith RW, Seymour CB, Mothersill CE. 2008. Dilution of irradiated cell conditioned medium and the bystander effect. Radiation Research 169(2):188-196.

99. Schoenherr D, Krueger SA, Martin L, Marignol L, Wilson GD, Marples B. 2013. Determining if low dose hyper-radiosensitivity (HRS) can be exploited to provide a therapeutic advantage: a cell line study in four glioblastoma multiforme (GBM) cell lines. International Journal of Radiation Biology 89(12):1009-1016.

100. Scott BR. 2008. It's time for a new low-dose-radiation risk assessment paradigm--one that acknowledges hormesis. Dose-response : a publication of International Hormesis Society 6(4):333-351.

101. Semenza GL. 2012. Hypoxia-inducible factors: mediators of cancer progression and targets for cancer therapy. Trends in Pharmacological Sciences 33(4):207-214.

102. Sethu S, Mendez-Corao G, Melendez AJ. 2008. Phospholipase D1 plays a key role in TNF-alpha signaling. Journal of Immunology 180(9):6027-6034.

103. Short SC, Woodcock M, Marples B, Joiner MC. 2003. Effects of cell cycle phase on low-dose hyper-radiosensitivity. International Journal of Radiation Biology 79(2):99-105.

104. Sinclair WK. 1968. Cyclic x-ray responses in mammalian cells in vitro. Radiation Research 33(3):620-643.

105. Song CW, Levitt SH, Park H. 2011. Response to "Stereotactic ablative radiotherapy in the framework of classical radiobiology: response to Drs. Brown, Diehn, and Loo." (Int J Radiat Oncol Biol Phys 2011;79:1599-1600) and "Influence of tumor hypoxia on stereotactic ablative radiotherapy (SABR): response to Drs. Mayer and Timmerman." (Int J Radiation Oncol Biol Phys 2011;78:1600). International Journal of Radiation Oncology, Biology, Physics 81(4):1193; author reply 1193-1194.

106. Sont WN, Zielinski JM, Ashmore JP, Jiang H, Krewski D, Fair ME, Band PR, Letourneau EG. 2001. First analysis of cancer incidence and occupational radiation exposure based on the National Dose Registry of Canada. American Journal of Epidemiology 153(4):309-318.

107. Srivastava K, Srivastava A, Kumar A, Mittal B. 2011. Gallbladder cancer predisposition: a multigenic approach to DNA-repair, apoptotic and inflammatory pathway genes. PloS One 6(1):e16449.

108. Stagni V, Oropallo V, Fianco G, Antonelli M, Cina I, Barila D. 2014. Tug of war between survival and death: exploring ATM function in cancer. International Journal of Molecular Sciences 15(4):5388-5409.

109. Symington LS. 2014. End Resection at Double-Strand Breaks: Mechanism and Regulation. Cold Spring Harbor Perspectives in Biology 6:a016436(8).

110. Tanooka H. 2001. Threshold dose-response in radiation carcinogenesis: an approach from chronic beta-irradiation experiments and a review of non-tumour doses. International Journal of Radiation Biology 77(5):541-551.

111. Teicher BA, Holden SA, Ara G, Dupuis NP, Goff D. 1995. Restoration of tumor oxygenation after cytotoxic therapy by a perflubron emulsion/carbogen breathing. The Cancer Journal from Scientific American 1(1):43-48.

112. Terasima T, Tolmach LJ. 1963. X-ray sensitivity and DNA synthesis in synchronous populations of HeLa cells. Science 140(3566):490-492.

113. Thompson LH. 2012. Recognition, signaling, and repair of DNA double-strand breaks produced by ionizing radiation in mammalian cells: the molecular choreography. Mutation Research 751(2):158-246.

114. Tucker JD, Sorensen KJ, Chu CS, Nelson DO, Ramsey MJ, Urlando C, Heddle JA. 1998. The accumulation of chromosome aberrations and Dlb-1 mutations in mice with highly fractionated exposure to gamma radiation. Mutation research 400(1-2):321-335.

115. Tucker JD, Tawn EJ, Holdsworth D, Morris S, Langlois R, Ramsey MJ, Kato P, Boice JDJ, Tarone RE, Jensen RH. 1997. Biological dosimetry of radiation workers at the Sellafield Nuclear Facility. Radiation Research 148:216-226.

116. UNSCEAR. 2000. United Nations Scientific Committee on the Effects of Atomic Radiation: Sources and effects of ionizing radiation.

117. Vaupel P, Harrison L. 2004. Tumor hypoxia: causative factors, compensatory mechanisms, and cellular response. The Oncologist 9 Suppl 5:4-9.

118. Wilson GD. 2004. Radiation and the cell cycle, revisited. Cancer Metastasis Reviews 23(3-4):209-225.

119. Wouters BG, Skarsgard LD. 1997. Low-dose radiation sensitivity and induced radioresistance to cell killing in HT-29 cells is distinct from the "adaptive

response" and cannot be explained by a subpopulation of sensitive cells. Radiation Research 148(5):435-442.

120. Wouters BG, Sy AM, Skarsgard LD. 1996. Low-dose hypersensitivity and increased radioresistance in a panel of human tumor cell lines with different radiosensitivity. Radiation Research 146(4):399-413.

121. Wykes SM, Piasentin E, Joiner MC, Wilson GD, Marples B. 2006. Low-dose hyper-radiosensitivity is not caused by a failure to recognize DNA double-strand breaks. Radiation Research 165(5):516-524.

122. Xu B, Kim ST, Lim DS, Kastan MB. 2002. Two molecularly distinct G(2)/M checkpoints are induced by ionizing irradiation. Molecular and Cellular Biology 22(4):1049-1059.

123. Yonezawa M, Takeda A, Misonoh J. 1990. Acquired radioresistance after low dose X-irradiation in mice. Journal of Radiation Research 31(3):256-262.

124. Zaichkina SI, Rozanova OM, Aptikaeva GF, Achmadieva A, Klokov DY. 2004. Low doses of gamma-radiation induce nonlinear dose responses in Mammalian and plant cells. Nonlinearity in Biology, Toxicology, Medicine 2(3):213-221.

## ABSTRACT


**CYTOGENETIC ANALYSES OF LOW DOSE HYPER-RADIOSENSITIVITY IN HUMAN LYMPHOBLASTOID CELLS IRRADIATED WITH COBALT-60 GAMMA RADIATION**

by

**GNANADA S. JOSHI**

**December 2014**

**Advisor:** Dr. James D. Tucker

**Major:** Biological Science

**Degree:** Doctor or Philosophy

**Chapter 2:**

The dose-effect relationships of cells exposed to ionizing radiation are frequently described by linear quadratic (LQ) models over an extended dose range. However, many mammalian cell lines, when acutely irradiated in G2 at doses ≤ 0.3 Gy, show hyper-radiosensitivity (HRS) as measured by reduced clonogenic cell survival, thereby indicating greater cell lethality than is predicted by extrapolation from high-dose responses. We therefore hypothesized that the cytogenetic response in G2 cells to low doses would also be steeper than predicted by LQ extrapolation from high doses. We tested our hypothesis by exposing four normal human lymphoblastoid cell lines to 0 – 400 cGy of Cobalt-60 gamma radiation. The cytokinesis block micronucleus assay was used to determine the frequencies of micronuclei and nucleoplasmic bridges. To characterize the dependence of the cytogenetic damage on dose, univariate and multivariate regression analyses were used to compare the responses in the low- (HRS) and high-dose response regions. Our data indicate that the slope of the response for all

four cell lines at ≤ 20 cGy during G2 is greater than predicted by an LQ extrapolation from the high-dose responses for both micronuclei and bridges. These results suggest that the biological consequences of low-dose exposures could be underestimated and may not provide accurate risk assessments following such exposures.

**Chapter 3:**

Low-dose hyper-radiosensitivity (HRS) has been reported in normal human lymphoblastoid cell lines for exposures at ≤ 20 cGy, but the cytogenetic effects of oxygen ($O_2$) levels in tissue culture media on HRS have not been evaluated. We asked whether HRS was lost in G2-irradiated cells grown in atmospheres of 2.5% or 5% $O_2$, compared to responses by cells cultured in ambient (~21%) $O_2$. The results indicate a loss of HRS when cells are cultured and irradiated either in 2.5% or 5% $O_2$. We then evaluated whether low $O_2$ levels either before or after exposure were responsible for the loss of HRS. For cells irradiated in an atmosphere of 5% $O_2$, subsequent immediate re-oxygenation to ambient $O_2$ levels restored the HRS effect, while cells cultured and irradiated at ambient $O_2$ levels and then transferred to 5% $O_2$ exhibited little or no HRS, indicating that ambient $O_2$ levels after, but not before, radiation substantially affect the amounts of cytogenetic damage. HRS was not observed when cells were irradiated in G1. At doses of 40 – 400 cGy there was significantly less cytogenetic damage when cells were recovering from radiation at low $O_2$ levels than at ambient $O_2$ levels. Here we provide the first cytogenetic evidence for the loss of HRS at low $O_2$ levels in G2-irradiated cells; these results suggest that at low $O_2$ levels for all doses evaluated there

is either less damage to DNA, perhaps due to lower amounts of reactive oxygen species, or that DNA damage repair pathways are activated more efficiently.

## AUTOBIOGRAPHICAL STATEMENT

## GNANADA S. JOSHI (nee KULKARNI)

### EDUCATION

**2009 – 2014** Ph.D. in Biological Science, Wayne State University, Detroit, MI, USA

**2004 – 2006** M.S. in Biotechnology, Wayne State University, Detroit, MI, USA

**2003 – 2004** Undergraduate course work towards graduate school admission requirements, Wayne State University, Detroit, MI, USA

**1992 – 1995** B.S. combined major: Botany, Zoology and Chemistry
Osmania University, Hyderabad, Andhra Pradesh, India

### AWARDS AND HONORS

- Student and New Investigator Travel Award, Environmental Mutagenesis and Genomics Society, 2013
- Student and New Investigator Travel Award, Environmental Mutagen Society, 2012
- Graduate Teaching Assistant award, Wayne State University, 2012
- Cover Picture for Mutation Research Reviews, 2011
- Second prize at the Annual Biological Sciences Poster Day, Wayne State University, 2005.
- Merit Scholarship (paid for Undergraduate studies), Indian Railways, 1992 to 1995

### PUBLICATIONS

1. Gebert N*, Joshi AS*, Kutik S*, Becker T, McKenzie M, Guan XL, Mooga VP, Stroud DA, **Kulkarni G**, Wenk MR, Rehling P, Meisinger C, Ryan MT, Wiedemann N, Greenberg ML, Pfanner N. Mitochondrial cardiolipin involved in outer-membrane protein biogenesis: implications for Barth syndrome. Current Biology 2009 Dec 29; 19(24): 2133-9.

2. **Joshi GS**, Joiner MC, Tucker, JD. Cytogenetic analyses of low dose hyper-radiation sensitivity in Cobalt 60 irradiated human lymphoblastoid cells. (*Submitted in July 2014*)

3. **Joshi GS**, Joiner MC, Tucker, JD. Cytogenetic analyses of low dose hyper-radiation sensitivity in Cobalt 60 irradiated human lymphoblastoid cells at low oxygen levels. (*Submitted in August 2014*)